© 2019. Published by The Company of Biologists Ltd | Journal of Cell Science (2019) 132, jcs236018. doi:10.1242/jcs.236018

RESEARCH ARTICLE

A novel interplay between GEFs orchestrates Cdc42 activity during cell polarity and cytokinesis in fission yeast

Brian S. Hercyk, Julie Rich-Robinson, Ahmad S. Mitoubsi, Marcus A. Harrell and Maitreyi E. Das*

ABSTRACT

Cdc42, a conserved regulator of cell polarity, is activated by two GEFs, Gef1 and Scd1, in fission yeast. Why the cell needs two GEFs is unclear, given that they are partially redundant and activate the same GTPase. Using the GEF localization pattern during cytokinesis as a paradigm, we report a novel interplay between Gef1 and Scd1 that spatially modulates Cdc42. We find that Gef1 promotes Scd1 localization to the division site during cytokinesis through recruitment of the scaffold protein Scd2, via a Cdc42 feedforward pathway. Similarly, during interphase Gef1 promotes Scd1 recruitment at the new end to enable the transition from monopolar to bipolar growth. Reciprocally, Scd1 restricts Gef1 localization to prevent ectopic Cdc42 activation during cytokinesis to promote cell separation, and to maintain cell shape during interphase. Our findings reveal an elegant regulatory pattern in which Gef1 primes Cdc42 activation at new sites to initiate Scd1-dependent polarized growth, while Scd1 restricts Gef1 to sites of polarization. We propose that crosstalk between GEFs is a conserved mechanism that orchestrates Cdc42 activation during complex cellular processes.

This article has an associated First Person interview with the first author of the paper.

KEY WORDS: Cdc42, GEF, Scd1, Gef1, Polarity, Cytokinesis

INTRODUCTION

Growth and division, fundamental processes in all cells, are essential for proper function and proliferation, and function through polarization. Cell polarization relies on the ability of the cytoskeleton to establish unique domains at the cell cortex to govern the local function and activity of specific proteins (Drubin and Nelson, 1996; Nance and Zallen, 2011). The Rho family of small GTPases serves as the primary regulators of cell polarity via actin regulation (Ridley, 2006). Although Rho GTPases have numerous functions, regulation of actin cytoskeleton organization is a prominent feature of these proteins. GTPases are active when GTP-bound and inactive once they hydrolyze GTP to GDP. Guanine nucleotide exchange factors (GEFs) activate GTPases by promoting the binding of GTP, while GTPase activating proteins (GAPs) inactivate GTPases by promoting GTP hydrolysis (Bos et al., 2007). A member of the Rho family of GTPases, Cdc42, is a master regulator of polarized cell growth and membrane trafficking in eukaryotes (Estravís et al., 2012, 2011; Etienne-Manneville, 2004; Harris and Tepass, 2010; Johnson, 1999). Cdc42 acts as a binary molecular switch and can respond to and initiate multiple signaling pathways. In most eukaryotes, Cdc42 is regulated by numerous GEFs and GAPs, complicating our understanding of GTPase regulation (Bos et al., 2007). In the fission yeast *Schizosaccharomyces pombe*, Cdc42 is activated by two GEFs, Gef1 and Scd1 (Chang et al., 1994; Coll et al., 2003). The presence of only two Cdc42 GEFs, and the well-documented process of cell polarization in these cells, make fission yeast an excellent model system to understand the mechanistic details of cell shape establishment. Here, we report that the two Cdc42 GEFs regulate each other during both cytokinesis and polarized growth. This finding provides new insights into the spatiotemporal regulation of Cdc42 during critical cellular events.

Fission yeast cells are rod-shaped and grow in a polarized manner from the two ends. Cells in early G2 phase are monopolar, and grow from the old end, which existed in the previous generation. Cells transition to a bipolar growth pattern in late G2 through the process of new end take-off (NETO), when growth initiates at the new end, which was formed during sister cell separation (Mitchison and Nurse, 1985). Due to this simple growth pattern, fission yeast is an excellent model to understand how a cell regulates polarized growth from multiple sites. In fission yeast, active Cdc42 displays anti-correlated oscillations between the two ends. The regulation that leads to this oscillatory pattern arises from both positive and time-delayed negative feedback, as well as from competition between the two ends, and controls cell shape and polarity (Das et al., 2012).

Cdc42 is activated at the cell ends to promote polarized growth and restricted from the cell sides to maintain cell shape (Das et al., 2012, 2015, 2009). Cdc42 is also involved in cytokinesis. During cytokinesis, Cdc42 activation promotes septum formation, and like in other systems, Cdc42 needs to be subsequently inactivated to promote cell separation (Atkins et al., 2013; Onishi et al., 2013; Wei et al., 2016). The regulatory mechanisms that allow for these spatiotemporal activation patterns are not well understood. To explain Cdc42 activation during polarized growth, it is important to first understand how Cdc42 regulators function. Gef1 and Scd1 are partially redundant but exhibit unique phenotypes when deleted (Chang et al., 1994; Coll et al., 2003), indicating that they may regulate Cdc42 in distinct, but overlapping, manners. Scd1 oscillates between the two cell ends, much like active Cdc42 (Das et al., 2012), and is essential for polarity establishment (Chang et al., 1994). Scd1 is also required for mating (Bendezú and Martin, 2013). In contrast, *gef1* mutants are narrower and grow in a monopolar manner (Coll et al., 2003; Das et al., 2012). Given that Gef1 is sparsely localized to the cortex (Das et al., 2015; Tay et al., 2018) and not required for polarity establishment, it is unclear why Gef1 is required for bipolar growth.

Investigations into the behaviors of Gef1 and Scd1 during interphase are complicated since Gef1 is barely detectable at sites of polarized growth, overlapping with Scd1. However, these GEFs also localize to the site of cell division during cytokinesis (Wei et al., 2016). The temporal localization and function of the two

Department of Biochemistry & Cellular and Molecular Biology, University of Tennessee, Knoxville, TN 7996-1939, USA.

*Author for correspondence (mdas@utk.edu)

M.E.D., 0000-0001-9164-0158

Received 4 July 2019; Accepted 4 November 2019

Journal of Cell Science (2019) 132, jcs236018. doi:10.1242/jcs.236018

GEFs are discernible during cytokinesis as they are recruited to the division site in succession to activate Cdc42. During cytokinesis, Gef1 localizes first to the actomyosin ring to activate Cdc42 and promote ring constriction (Wei et al., 2016). Next, Scd1 localizes to the ingressing membrane and regulates septum formation (Wei et al., 2016). The temporal difference between Gef1 and Scd1 localization at the division site enables investigation of the significance of the GEFs in Cdc42 regulation, which is unclear from studies solely of the growing ends.

Bipolar growth occurs when the new end is able to overcome the dominance of the old end. Here, we show that Gef1 enables the new end to overcome old end dominance and promote bipolar growth. We find that in *gef1* mutants both the Cdc42 GEF Scd1 and its scaffold Scd2 are localized mainly to the old ends. Using cytokinesis as a paradigm we identify a novel crosstalk between Gef1 and Scd1. Our data indicate that Gef1 promotes the localization of Scd1 to the division site via Cdc42 activation and the scaffold Scd2. Gef1 activates Cdc42, which then promotes recruitment of Scd2, and consequently of Scd1. We extend these observations to the sites of polarized growth, where we show that Gef1 promotes bipolar Scd1 and Scd2 localization to initiate growth at a second site, while Scd1 prevents ectopic Gef1 localization to the division site and the cell cortex. By this manner of regulation, Cdc42 activation is promoted at the new end of the cell with no prior growth history, but is restricted from random sites. To our knowledge, such crosstalk has not been reported to function between GEFs of the same GTPase. The interplay between the Cdc42 GEFs operates in the same manner during both cytokinesis and polarized growth, suggesting that this is a conserved feature of Cdc42 regulation.

RESULTS

Gef1 promotes Scd1 recruitment to the division site

We have reported that the GEF Scd1 localizes to the membrane adjacent to the actomyosin ring after Gef1 to activate Cdc42 along the membrane barrier (Wei et al., 2016). Since Scd1 arrives at the division site soon after Gef1, it is possible that Gef1 promotes Scd1 localization. Alternatively, if Gef1 and Scd1 act independently, then loss of *gef1* would not impact Scd1 localization to the division site. To test this, we examined whether Scd1 localization to division site is Gef1-dependent. Both Gef1 and Scd1 are low-abundance proteins and are not suitable for live cell imaging over time. To overcome this limitation, we used the actomyosin ring as a temporal marker. The actomyosin ring undergoes visibly distinct phases during cytokinesis: assembly, maturation, constriction and disassembly. We determined the timing of protein localization to the division site by comparing it to the corresponding phase of the actomyosin ring. We have previously reported that ring constriction is delayed in *gef1Δ* mutants (Wei et al., 2016). To eliminate any bias in protein localization resulting from this delay, we only analyzed cells in which the rings had initiated constriction. In *gef1Δ* mutants, the number of constricting rings that recruited Scd1–3×GFP decreased to 15% from 96% in *gef1+* cells (Fig. 1A,B, $P<0.0001$; Fig. S1A–C). Furthermore, the *gef1Δ* cells that managed to recruit Scd1–3×GFP did not do so as efficiently as *gef1+* cells, given the 15% decrease in Scd1–3×GFP fluorescence intensity at the division site (Fig. 1A,C, $P=0.0089$; Fig. S1D–F). This indicates that Gef1 promotes Scd1 localization to the division site and that the two GEFs are not independent.

Constitutively active Cdc42 is sufficient to restore Scd1 to the division site in *gef1Δ* mutants

Next, we investigated how Gef1 promotes Scd1 recruitment to the division site. GEF recruitment to sites of Cdc42 activity occurs via positive feedback, as reported in budding yeast (Butty et al., 2002; Irazoqui et al., 2003; Kozubowski et al., 2008; Witte et al., 2017). In this model, activation of Cdc42 leads to further recruitment of the scaffold protein BEM1, which then recruits the GEF CDC24 to the site of activity, thus helping to break symmetry and promote polarized growth. A similar positive feedback may also exist in fission yeast (Das et al., 2012; Das and Verde, 2013). Indeed, a recent study suggests that the scaffold Scd2 establishes positive feedback (Lamas et al., 2019 preprint). We hypothesized that Gef1-activated Cdc42 acts as a seed for Scd1 recruitment to the division site. To test this, we asked whether constitutive activation of Cdc42 could rescue the Scd1 recruitment defect exhibited by *gef1Δ* cells. For this approach to work, the constitutively active Cdc42 must localize to the division site. Localization of active Cdc42 is visualized via the bio-probe CRIB–3×GFP, which specifically binds GTP-Cdc42. Since our previous work reported that Cdc42 activity is reduced at the division site in *gef1Δ* cells (Wei et al., 2016), we validated this approach by first testing whether constitutively active Cdc42 restores CRIB–3×GFP localization at the division site in *gef1Δ* cells. The constitutively active allele *cdc42G12V* and the bio-probe CRIB–3×GFP were expressed in *gef1+* and *gef1Δ* cells. Mild expression of *cdc42G12V* was sufficient to restore CRIB–3×GFP intensity at the division site to physiological levels in *gef1Δ* cells (Fig. 1D,E, $P<0.0001$; Fig. S1G–I). Likewise, expression of *cdc42G12V* restored Scd1–tdTomato localization to the division site in *cdc42G12V gef1Δ* cells (Fig. 1F,G; Fig. S1J–L). This demonstrates that active Cdc42 can promote Scd1 recruitment. Next, we asked how active Cdc42 promotes Scd1 localization. We examined downstream targets of active Cdc42 for this purpose. The Cdc42 ternary complex consists of the GEF Scd1, the scaffold protein Scd2, and the downstream effector kinase Pak1 (also known as Shk1) (Endo et al., 2003). Observations in budding yeast suggest that the PAK kinase Cla4 mediates GEF recruitment (Kozubowski et al., 2008). Contrary to this hypothesis, we find that Scd1–3×GFP intensity increases in the *nmt1 switch-off* mutant allele of *pak1*, compared to *pak1+* cells (Fig. S2H). These findings support similar observations reported in the hypomorphic temperature-sensitive *pak1* allele, *orb2-34* (Das et al., 2012), and indicate that *pak1* does not facilitate Scd1 recruitment to the site of action.

Gef1 promotes Scd2 localization to the division site, which in turn recruits Scd1

The scaffold protein Scd2 is a component of the Cdc42 ternary complex that binds active Cdc42 (Endo et al., 2003; Wheatley and Rittinger, 2005). We hypothesized that Gef1-dependent active Cdc42 recruits Scd1 to the division site through the scaffold Scd2. Indeed, we find that *gef1Δ* cells displayed a significant decrease in Scd2–GFP-containing assembled rings compared to *gef1+* cells. In *gef1Δ* mutants, the number of rings that recruited Scd2–GFP prior to ring constriction decreased to 8% compared to 88% in *gef1+* cells, indicating a delay in Scd2 recruitment (Fig. 2A,B, $P>0.0001$; Fig. S2A–C). Although *gef1Δ* cells were able to recruit Scd2 to the division site once ring constriction began, the fluorescence intensity of Scd2–GFP at the division site was reduced by 61% compared to *gef1+* cells (Fig. 2A,C, $P>0.0001$; Fig. S2D, S2E–G). Gef1 thus promotes Scd2 localization to the division site. Since previous work indicates that Scd1 and Scd2 require each other for their localization, it is possible that a decrease in Scd2 at the division site observed in *gef1* mutants is due to a decrease in Scd1 at this site (Kelly and Nurse, 2011). However, contrary to previous findings, we observed that Scd2–GFP localization at the division site is not impaired in *scd1Δ* cells (Fig. 2D) (Kelly and Nurse, 2011). In

Journal of Cell Science (2019) 132, jcs236018. doi:10.1242/jcs.236018

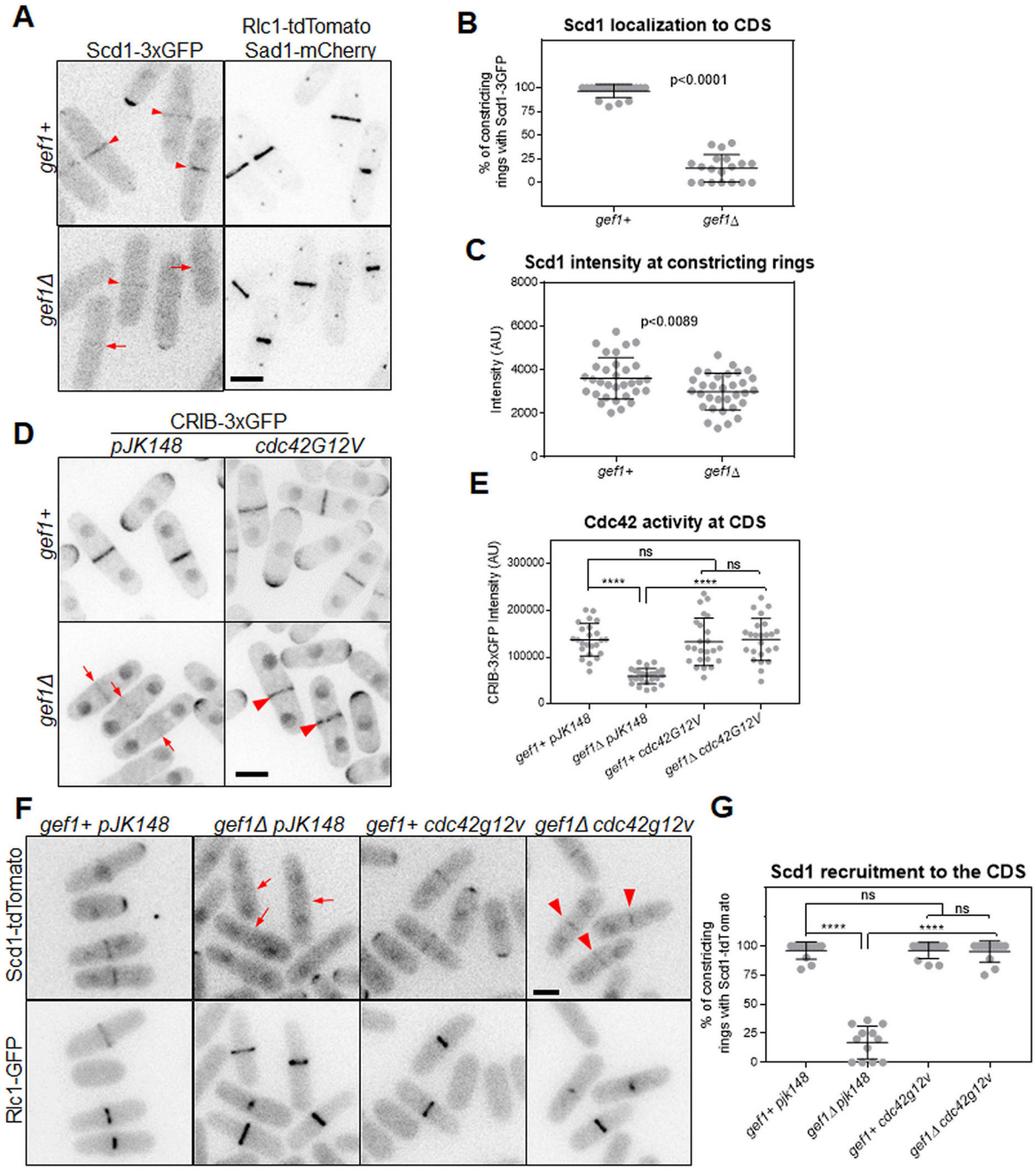

Fig. 1. Gef1-mediated Cdc42 activation recruits Scd1 to the division site. (A) Scd1–3×GFP localization in *gef1+* and *gef1Δ* cells expressing the ring and spindle pole body (SPB) markers Rlc1–tdTomato and Sad1–mCherry, respectively. Arrowheads, Scd1–3×GFP localized to the division site; arrows, constricting rings lacking Scd1–3×GFP. (B,C) Quantification of Scd1–3×GFP localization to the cell division site (CDS) (B) and intensity at constricting rings (C) in the indicated genotypes. (D) CRIB–3×GFP localization to the division site in *gef1+* and *gef1Δ* cells transformed with the control vector *pJK148* or *cdc42G12V*. Arrows, reduced CRIB–3×GFP signal at the division site; arrowheads, restored CRIB–3×GFP signal at the division site. (E) Quantification of CRIB–3×GFP intensity at the CDS in the indicated genotypes. (F) Scd1–tdTomato localization to constricting rings marked by Rlc1–GFP in *gef1+* and *gef1Δ* cells transformed with the control vector *pJK148* or *cdc42G12V*. Arrows, constricting rings lacking Scd1–tdTomato; arrowheads, restored Scd1–tdTomato at the constricting rings. (G) Quantification of cells with Scd1–tdTomato at the constricting rings of cells of the indicated genotypes. Each data point corresponds to the mean of an analyzed field of cells (n>5) from the same experiment. Black bars on data points show the mean±s.d. for each genotype. Significance determined by one-way ANOVA with Tukey's multiple comparisons post-hoc test; ****P<0.0001; ns, not significant. All images are inverted max projections. Scale bars: 5 µm.

contrast, Scd1–3×GFP localization is completely abolished at the division site in *scd2Δ* cells (Fig. 2E). Scd2 localization is independent of Scd1 and depends on Gef1 instead.

Taken together, our data reveal that Gef1 promotes Scd2 localization to the division site, which then recruits Scd1. Based on these data, we hypothesized that Gef1, Scd2 and Scd1 sequentially localize to the division site. To test this, we examined the temporal localization of these proteins to the division site. Since these proteins do not lend themselves to extended time lapse imaging, we used the spindle pole bodies as an internal timer. The

Journal of Cell Science (2019) 132, jcs236018. doi:10.1242/jcs.236018

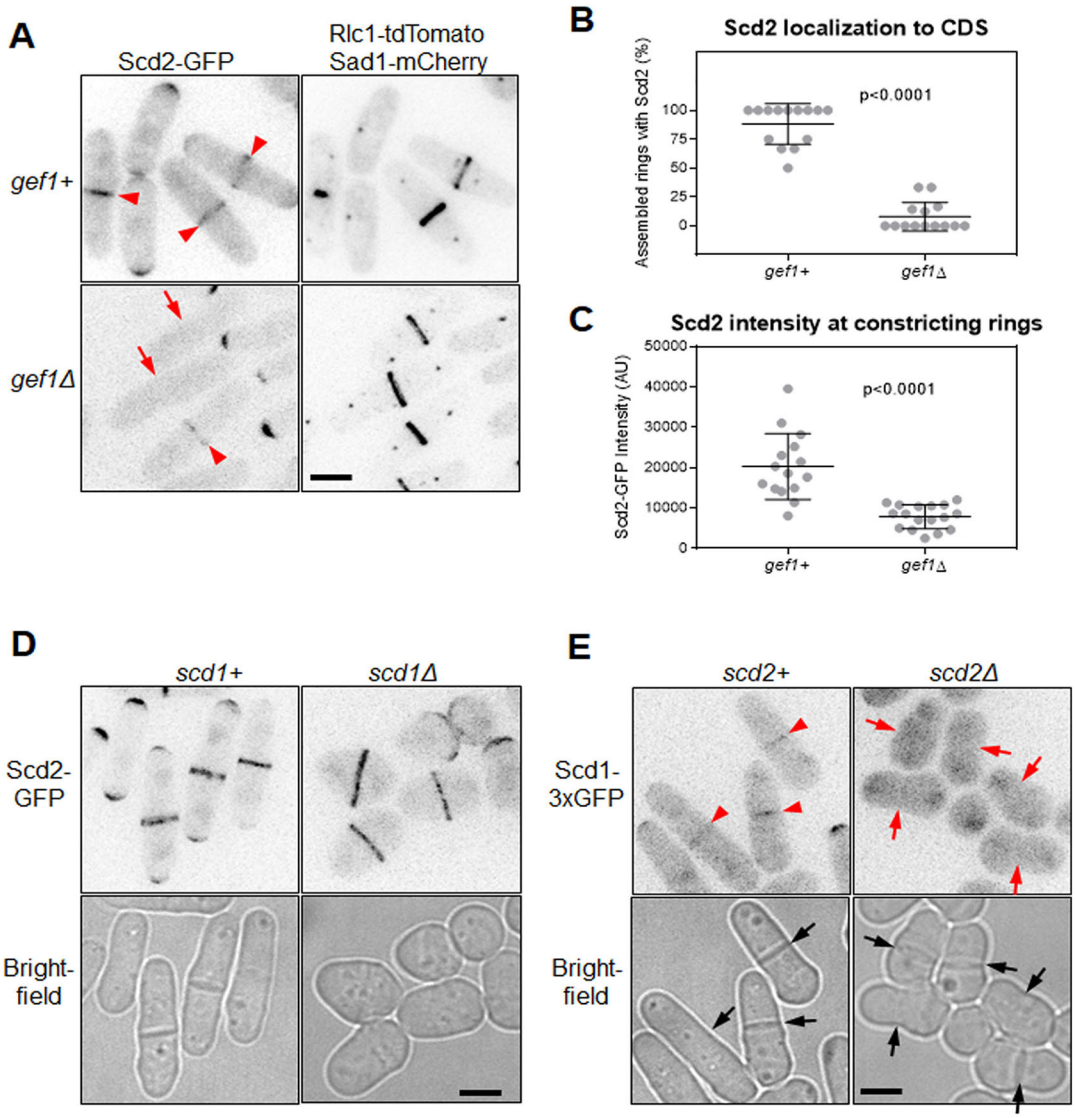

Fig. 2. Gef1 promotes Scd1 localization to the division site via the scaffold Scd2. (A) Scd2–GFP localization in *gef1+* and *gef1Δ* cells expressing the ring and spindle pole body (SPB) markers Rlc1–tdTomato and Sad1–mCherry. Arrowheads, Scd2–GFP localized to constricting rings; arrows, assembled rings lacking Scd2–GFP. (B,C) Quantification of Scd2–GFP localization to the CDS (B) and intensity at constricting rings (C) in the indicated genotypes. Each data point corresponds to the mean of an analyzed field of cells (n>5) from the same experiment. Black bars on data points show the mean±s.d. for each genotype. Significance determined by Student's t-test. (D) Scd2–GFP localization to the division site in *scd1+* and *scd1Δ* cells. (E) Scd1–3×GFP localization in *scd2+* and *scd2Δ* cells. Black arrows, division site; red arrowheads, Scd1–3×GFP at the division site; red arrows, absence of Scd1–3×GFP at the division site. All images are inverted max projections with the exception of bright field. Scale bars: 5 µm.

distance between spindle pole bodies is a well-established temporal marker to determine a cell's cytokinetic stage. The spindle pole body distance increases as mitosis progresses until the cell reaches anaphase B (Nabeshima et al., 1998), at which time the actomyosin ring starts to constrict (Wu et al., 2003). We report the spindle pole body distance at which Gef1–mNG (monomeric NeonGreen), Scd1–3×GFP and Scd2–GFP signals are visible at the division site before the actomyosin rings start constriction (Fig. 3A). Gef1–mNG and Scd2–GFP appear around the same time during mitosis with a mean spindle pole body distance of 5.9 µm, and 6.6 µm, respectively (Fig. 3B, not significant). Scd1–3×GFP arrives later with a longer mean spindle pole body distance of 7.6 µm (Fig. 3B, P=0.005). Furthermore, in cells expressing both Gef1–tdTomato and Scd2–GFP, 100% of assembled rings with Gef1 invariably also had Scd2 at the division site (Fig. 3C,D). In cells expressing Scd2–GFP and Scd1–tdTomato, only 59% of assembling rings localized both Scd2 and Scd1 (Fig. 3C,D). In cells expressing both Gef1–tdTomato and Scd1–3×GFP, 61% of assembling rings with Gef1 also had Scd1 (Fig. 3C,D). Taken together, this demonstrates that Gef1 recruits Scd2 to actomyosin rings prior to recruitment of Scd1.

Gef1 enables bipolar localization of Scd1 and Scd2 to the cell poles

To determine whether the Gef1-mediated regulation of Scd1 and Scd2 localization was conserved during cell polarity, we analyzed whether their localization at the cell poles was altered in *gef1Δ* mutants. Scd1 and Scd2, like active Cdc42, undergo oscillations between the two competing ends (Das et al., 2012); thus, a bipolar cell does not always display bipolar Scd1 or Scd2 localization. Fewer new ends in *gef1Δ* cells exhibited Scd1–3×GFP; bipolar Scd1–3×GFP was observed in 30% of interphase *gef1+* cells, but only in 14% of *gef1Δ* cells (Fig. 4A,B; P=0.0004; Fig. S3A–C).

Journal of Cell Science (2019) 132, jcs236018. doi:10.1242/jcs.236018

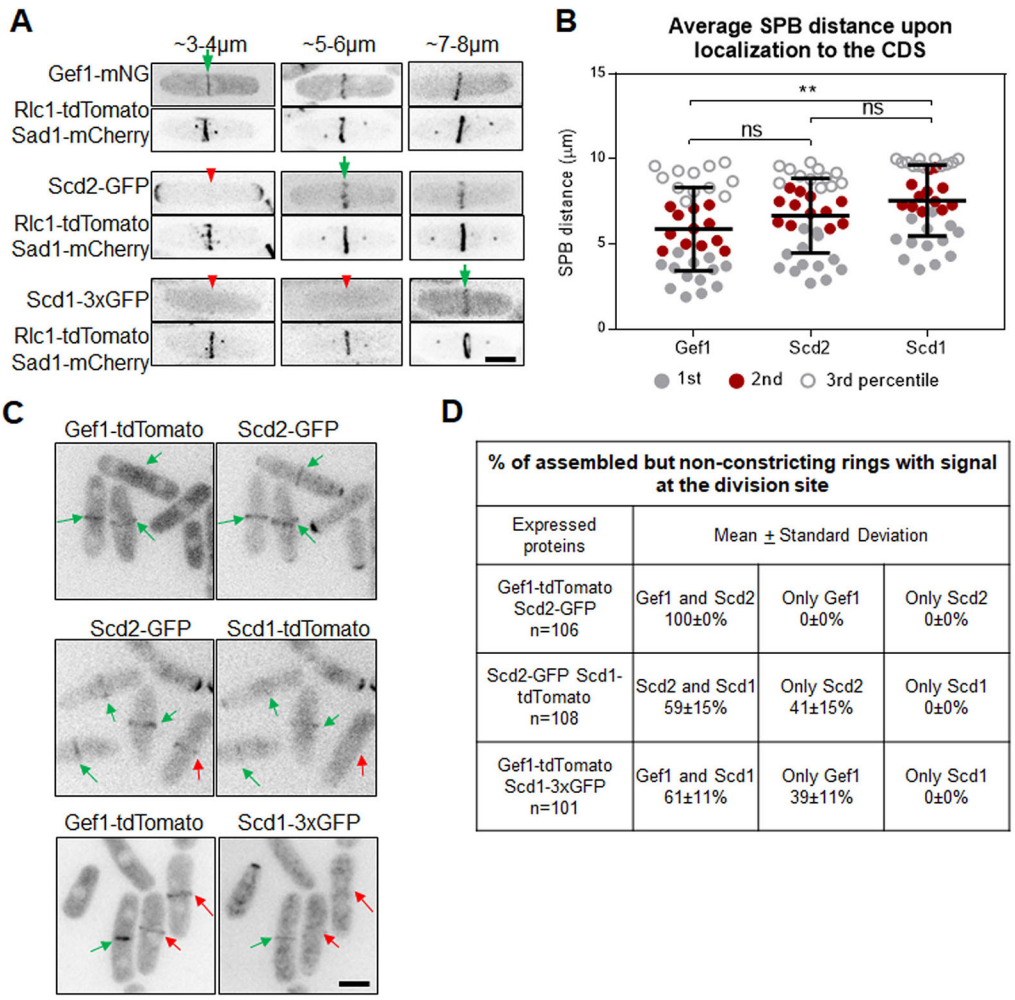

D

% of assembled but non-constricting rings with signal at the division site			
Expressed proteins	Mean ± Standard Deviation		
Gef1-tdTomato Scd2-GFP n=106	Gef1 and Scd2 100±0%	Only Gef1 0±0%	Only Scd2 0±0%
Scd2-GFP Scd1-tdTomato n=108	Scd2 and Scd1 59±15%	Only Scd2 41±15%	Only Scd1 0±0%
Gef1-tdTomato Scd1-3xGFP n=101	Gef1 and Scd1 61±11%	Only Gef1 39±11%	Only Scd1 0±0%

Fig. 3. Temporal localization of Gef1, Scd2 and Scd1 to the site of cell division. (A) Representative images showing the localizations of Gef1–mNG, Scd2–GFP and Scd1–3×GFP (upper panels) as a function of spindle pole body (SPB) distance (lower panels). Green arrows, smallest SPB distance at which signal is visible; red arrowheads, SPB distance prior to localization. (B) Quantification of Gef1, Scd2 and Scd1 localization to the CDS, with respect to SPB distance. Means of the distance between SPBs of the first 33rd percentile in early anaphase cells at which signal first appears (gray circles). Each data point corresponds to the mean of an analyzed field of cells (n>5) from the same experiment. Black bars on data points show the mean ±s.d. for each genotype. Significance determined by one-way ANOVA with Tukey's multiple comparisons post-hoc test; **P=0.005; ns, not significant. Second and third percentiles shown in red circles and white circles, respectively. (C) Representative images of early anaphase cells expressing combinations of Scd1–3×GFP, Gef1–tdTomato, Scd2–GFP and Scd1–tdTomato. Green arrows, sites of colocalization; red arrows, sites with only one of the proteins expressed. All images are inverted max projections. (D) Localization patterns of Gef1, Scd2 and Scd1 at the division site in cells coexpressing any two of these three fluorescently tagged proteins. Scale bars: 5 µm.

Similarly, 70% of *gef1+* cells displayed bipolar Scd2–GFP localization, but this was reduced to 30% in *gef1Δ* cells (Fig. 4A,B, P<0.0001; Fig. S3A–C). While this suggests that Gef1 promotes Scd1 and Scd2 localization to the new end to enable bipolar growth, this interpretation suffers from some complications. The old and new ends compete with each other for active Cdc42 (Das et al., 2012). It is possible that in *gef1Δ* mutants the new end fails to grow since the old end traps Scd1 and Scd2, resulting in monopolar distribution of these proteins. However, we did not find enhanced Scd1–3×GFP levels at the old end in *gef1Δ* cells compared to *gef1+* cells (Fig. S3D). This suggests that Gef1 does not prevent accumulation of Scd1 and Scd2 at the old ends.

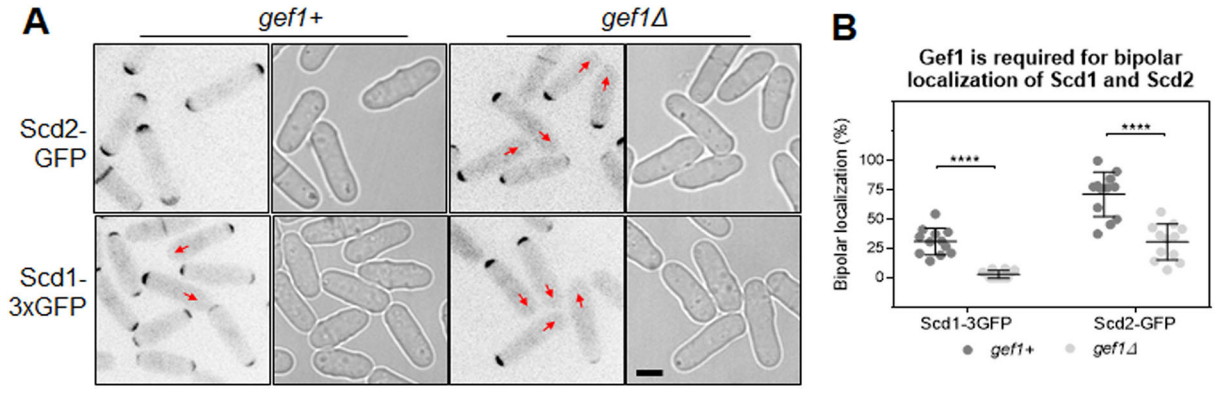

Fig. 4. Gef1 promotes localization of polarity factors Scd1 and Scd2 to the new end. (A) Scd2–GFP and Scd1–3×GFP localization to the sites of polarized growth in *gef1+* and *gef1Δ* cells. Arrows, new ends lacking Scd2–GFP or Scd1–3×GFP. All images are inverted max projections with the exception of bright field. Scale bar: 5 µm. (B) Quantifications of bipolar Scd1–3×GFP and Scd2–GFP localization in the indicated genotypes. Significance determined by one-way ANOVA with Tukey's multiple comparisons post-hoc test; ****P<0.0001. Reported P-values from Student's t-tests. Each data point corresponds to the mean of an analyzed field of cells (n>5) from the same experiment. Black bars on data points show the mean±s.d. for each genotype.

Journal of Cell Science (2019) 132, jcs236018. doi:10.1242/jcs.236018

Gef1 recruits Scd1 to the new end via Cdc42 activation

Next, we asked whether Gef1 recruits Scd1 to the new end via Cdc42 activation, just as it does at the division site. We first tested whether expression of constitutively active Cdc42 results in bipolar localization of active Cdc42 in *gef1Δ* cells, as indicated by CRIB–3×GFP localization. Low-level expression of *cdc42G12V* was sufficient to restore bipolar CRIB–3×GFP localization in *gef1Δ* cells, compared to the empty-vector-containing *gef1Δ* mutants (Fig. 5A,B, $P<0.0001$; Fig. S4A–C). We observed bipolar CRIB–3×GFP in 35% of *gef1+* cells transformed with the empty vector *pJK148* and in 36% of cells expressing *cdc42G12V*. In *gef1Δ pJK148* mutants 8% of cells displayed bipolar CRIB–3×GFP. In contrast, in *gef1Δ cdc42G12V* cells, bipolar CRIB–3×GFP was restored to 34%. In the same cells, we observed bipolar Scd1–tdTomato in 21% of *gef1+ pJK148* cells, and in 23% of cells expressing *cdc42G12V*. In *gef1Δ pJK148* mutants, we observed bipolar Scd1–tdTomato in only 6% of cells. Furthermore, in *gef1Δ cdc42G12V* cells, bipolar Scd1–tdTomato was restored to 19% (Fig. 5A,C; Fig. S4D–F). Thus, expression of *cdc42G12V* was sufficient to restore bipolar Scd1–tdTomato localization to the cell ends in *gef1Δ* mutants, just as it was at the division site (Fig. 5A,C). This demonstrates that Gef1 promotes Scd1 localization to the new ends through Cdc42 activation.

Next, we asked whether bipolar localization of Scd1–tdTomato correlated with bipolar growth. To determine this, we stained cells with Calcofluor to mark the sites of polarized growth. Bipolar growth was exhibited in 40% of *gef1+ pJK148* cells and 14% of *gef1Δ pJK148* mutants ($P<0.0001$, Fig. S5). Expression of *cdc42G12V* in *gef1+* and *gef1Δ* cells elevated bipolarity to 49% and 48%, respectively ($P<0.0001$, Fig. S5). To address whether cells grew at poles that contained high levels of Scd1–tdTomato, we examined the growth pattern of cells exhibiting bipolar or monopolar Scd1–tdTomato localization through time-lapse microscopy. Regardless of genotype, all cells with bipolar Scd1–tdTomato localization grew in a bipolar manner (Fig. S6). Approximately 20% of *gef1+ pJK148*, *gef1+ cdc42G12V* and *gef1Δ cdc42G12V* cells, and 9% of *gef1Δ pJK148* mutants with monopolar Scd1–tdTomato grew in a bipolar manner (Fig. S6). That

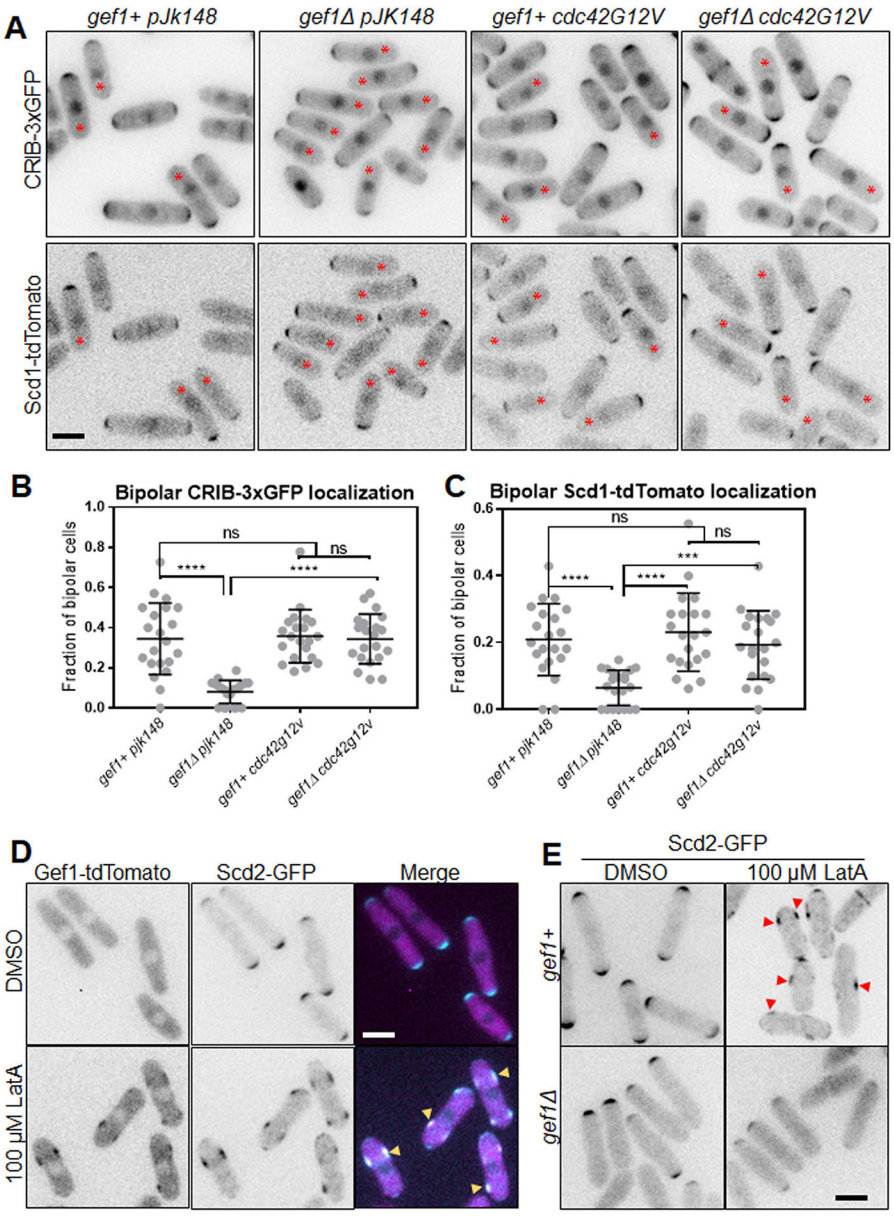

Fig. 5. Gef1 promotes Scd1 localization to the new end via Cdc42 activation. (A) CRIB–3×GFP and Scd1–tdTomato localization at cell tips, in *gef1+* and *gef1Δ* cells transformed with the control vector *pJK148* or *cdc42G12V*. Asterisks indicate the new end of monopolar cells. (B,C) Quantification of the percent of cells that exhibit bipolar CRIB–3×GFP (B) and Scd1–tdTomato (C) localization at cell tips in the indicated genotypes. Significance determined by one-way ANOVA with Tukey's multiple comparisons post-hoc test; ***$P<0.001$, ****$P<0.0001$; ns, not significant. Each data point corresponds to the mean of an analyzed field of cells ($n>5$) from the same experiment. Black bars on data points show the mean±s.d. for each genotype. (D) Localization of Gef1–tdTomato and Scd2–GFP in DMSO- or LatA-treated cells. (E) Localization of Scd2–GFP in *gef1+* and *gef1Δ* cells treated with DMSO or LatA. Arrowheads, ectopic Scd2-GFP. All images are inverted max projections with the exception of bright field unless specified. Scale bars: 5 µm.

Journal of Cell Science (2019) 132, jcs236018. doi:10.1242/jcs.236018

a fraction of cells grow in a bipolar manner even though Scd1–tdTomato appears monopolar could be due to oscillation of Scd1 between the two ends in bipolar cells (Das et al., 2012). Since Scd1–tdTomato fluorescence was only captured at time 0, it is likely that in these cells the signal was detected during the transition of Scd1–tdTomato from one end to the other. While Scd1 requires Scd2 for its localization, Scd2 localization is independent of Scd1 (Fig. S4G). Scd2 likely binds active Cdc42, so it is possible that Gef1-mediated Cdc42 activation leads to Scd2 recruitment. To test this, we monitored ectopic Gef1 localization. In cells treated with the actin-depolymerizing drug latrunculin A (LatA), Gef1–tdTomato ectopically localizes to the cell sides (Fig. 5D). In these cells, Scd2–GFP colocalizes with ectopic Gef1–tdTomato at the cell sides. Moreover, in *gef1Δ* cells Scd2–GFP fails to localize to the cell sides upon LatA treatment (Fig. 5E). In these cells, Scd2–GFP remains at the cell ends, but the levels are much reduced. This provides further evidence that Gef1 marks the site for Scd2 recruitment at the cell cortex.

Gef1 enables the transition from monopolar to bipolar growth

Fission yeast transitions from monopolar to bipolar growth upon reaching a certain size (Mitchison and Nurse, 1985). It has been proposed that this size requirement is necessary to establish two stable regions of Cdc42 activity (Das et al., 2012). Because protein abundance scales with cell size, growth may allow for the accumulation of sufficient GEFs and other polarity factors to maintain two sites of Cdc42 activity (Das et al., 2012). These models suggest that in *gef1Δ* cells the total active Cdc42 levels are insufficient to allow bipolar growth, thus resulting in monopolarity. However, the dependence of bipolarity on cell size and protein abundance cannot be explained in G1-arrested *cdc10-129* mutants (Marks et al., 1986). *cdc10-129* cells shifted to 36°C remain monopolar even as they grow longer compared to *cdc10+* cells (Fig. 6A).

To gain insight into the transition to bipolar growth we examined the growth patterns of *gef1Δ* mutants. The old ends initiate growth immediately after completion of division, and upon reaching a certain size the new end initiates growth, resulting in bipolarity (Fig. 6B) (Mitchison and Nurse, 1985). The two ends compete for active Cdc42; at first the old end, which is dominant, wins this competition (Das et al., 2012). A growth pattern in which one daughter cell is monopolar and the other daughter cell is prematurely bipolar is exhibited in 68% of monopolar *gef1Δ* mutant cells (Fig. 6C; Fig. S6A). In monopolar *gef1Δ* cells, growth occurs at the old end, which grew in the previous generation (Fig. 6C; Fig. S7A). The new end frequently fails to grow since it cannot overcome the old end's dominance. The daughter cell that inherits its parent cell's non-growing end typically displays precocious bipolar growth, indicating that these cells do not contain a dominant end. This suggests that a cell end is dominant if it grew in the previous generation. These results indicate that the new ends of *gef1Δ* cells are not well-equipped to overcome old end dominance. To further confirm this, we tracked the fate of cell ends with a known history of growth in *gef1+* and *gef1Δ* cells. In *gef1+* cells, 97% of daughter cells derived from a growing end display a normal growth pattern (Fig. 6D). In *gef1Δ* cells, 81% of daughter cells derived from a growing end failed to initiate growth at their new end and were thus monopolar (Fig. 6D). These data indicate that Gef1 enables the new end to overcome old end dominance to promote bipolar growth. Furthermore, our data indicate that Gef1 promotes bipolarity by promoting Scd1 localization to the new end. As a further test, we asked whether Scd1 localization would be enhanced at the new end in the precociously bipolar *gef1S112A* mutant, in which Gef1S112A constitutively localizes to the cortex. Indeed, 52% of *gef1S112A* cells show bipolar Scd1–3×GFP localization, while this is seen in only 33% of *gef1+* cells (Fig. S7B,C, $P<0.0001$).

Scd1 prevents ectopic Gef1 localization to the cell cortex and the division site

Cells treated with LatA show ectopic Cdc42 activation at the cell sides (Mutavchiev et al., 2016). As reported earlier (Kelly and Nurse, 2011), we find that LatA treatment leads to a severe loss in Scd1–mNG levels at the cell ends and at the site of cell division (Fig. S8G). We asked whether ectopic Gef1 localization in LatA-treated cells results from loss of Scd1 from the cell cortex. To test this, we analyzed Gef1–mNG localization in *scd1Δ* mutants. In *scd1+* cells, Gef1–mNG is mostly cytoplasmic and displays sparse but polarized localization at cell ends (Fig. 7Ai). In *scd1Δ* mutants, Gef1–mNG shows depolarized cortical localization with random patches at the cortex like that in *scd1+* cells treated with LatA (Fig. 7Aii,v). Gef1–mNG localization in *scd1Δ* cells treated with LatA is similar to that in untreated *scd1Δ* cells (Fig. 7Aii,vi). This suggests that Scd1 is required to prevent ectopic Gef1 localization and restricts it to the cell ends.

Next, we asked whether ectopic Gef1 in *scd1Δ* cells and in LatA-treated cells leads to ectopic Cdc42 activation. We find that active Cdc42 appears depolarized in *scd1Δ* mutants during interphase. While CRIB–3×GFP remains restricted to the ends in *scd1+* cells, in *scd1Δ* mutants it appears localized to random patches at the cortex (Fig. 7Bi,ii). LatA treatment leads to ectopic CRIB localization (Mutavchiev et al., 2016) and we observed that ectopic CRIB–3×GFP is abolished in *gef1Δ* cells (Fig. 7Bvii,ix). In *gef1Δ* cells treated with LatA, CRIB–3×GFP remains at the cell ends, but at lower levels compared to untreated cells. This indicates that Scd1 is functionally epistatic to actin in the removal of Gef1 from the cell cortex. Taken together, these data demonstrate that Scd1 at the cell ends prevents ectopic Gef1 localization and Cdc42 activation. This observation is supported by previous work, in which deletion of *gef1* restores polarized growth in cells expressing only minimal levels of *scd1* (Tay et al., 2018).

Because we find that Scd1 regulates Gef1 localization at sites of polarized growth, we asked whether a similar relationship also occurs at the division site. To test this, we analyzed Gef1 localization in *scd1Δ* mutants. We observed persistent Gef1 localization in *scd1* mutants after ring constriction. In *scd1Δ* mutants, after completion of ring constriction and disassembly, Gef1 remains at the membrane that was adjacent to the ring (Fig. 7C). Among *scd1Δ* cells that had completed constriction, 70% show persistent Gef1–mNG at the newly formed membrane barrier, as confirmed by the absence of Rlc1–tdTomato (Fig. 7C,D; Fig. S8A–C). Similar Gef1–mNG localization was observed in only 20% of *scd1+* cells (Fig. 7C,D, $P<0.0001$; Fig. S8A–C).

We find that Gef1–mNG removal from the division site is also dependent on actin. We analyzed Gef1 localization in cells with an actin cytoskeleton disrupted via LatA treatment. In LatA-treated cells that were fully septated following completion of ring constriction, we observed persistent Gef1 localization at the division site. Gef1–mNG persists on both sides of the septum barrier in 40% of cells treated with LatA, but not in mock DMSO-treated cells (Fig. 7E,F; Fig. S8D–F). This demonstrates that the actin cytoskeleton promotes Scd1 localization and that Scd1 promotes Gef1 removal from the division site. To confirm that actin promotes Gef1 removal via Scd1, we looked for a functional epistatic relationship between Scd1 and actin. We treated *scd1+* and

Journal of Cell Science (2019) 132, jcs236018. doi:10.1242/jcs.236018

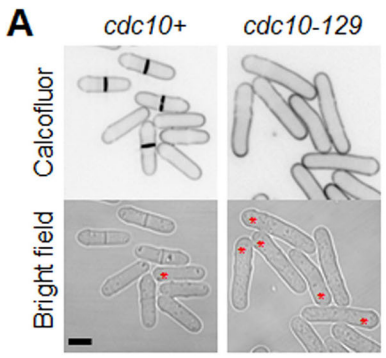

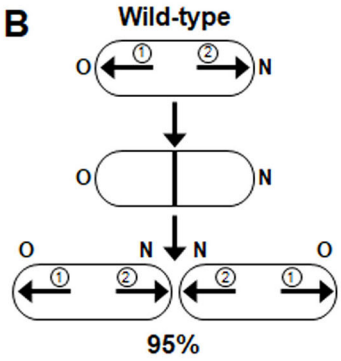

D Polarity of cells derived from ends that grew in the previous generation

	gef1+ (n=39)	*gef1Δ* (n=74)
monopolar	3%	81%
NETO	97%	9%
precociously bipolar	0%	9%

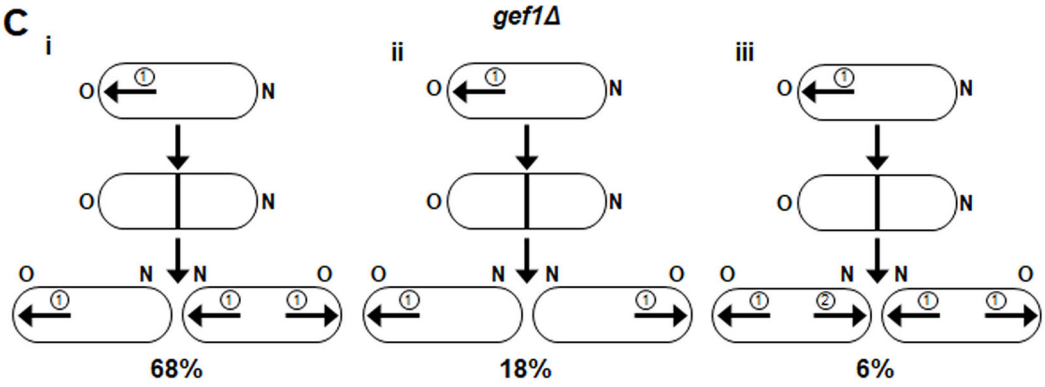

Fig. 6. Gef1 promotes bipolar growth via new end take-off. (A) Polarized growth phenotypes of Calcofluor-stained *cdc10+* and *cdc10-129* cells grown at 36°C. *cdc10+* cells initiate bipolar growth, while *cdc10-129* cells arrest at G1 and remain monopolar. Asterisks mark cells that exhibit monopolar growth. Scale bar: 5 µm. (B) Wild-type cells predominately display old-end (O) growth, followed by a delayed onset of new-end growth (N). (C) i. In *gef1Δ* mutants, 68% of monopolar cells yield a monopolar daughter cell from the end that grew in the previous generation and a bipolar daughter cell from the end that failed to grow in the previous generation. ii.18% of monopolar cells yield two monopolar cells. iii. 6% of monopolar cells yield two monopolar cells. Circled numbers describe the order of growth. Arrows correspond to direction of growth. (D) Percentage polarity of cells derived from ends that grew in the previous generation in *gef1+* and *gef1Δ* cells. NETO, new end take-off.

scd1Δ cells expressing Gef1–mNG with LatA or DMSO. In cells treated with DMSO, Gef1–mNG persists in 20% of septated *scd1+* cells and in 63% of septated *scd1Δ* cells. In cells treated with LatA, Gef1–mNG persists in 40% of septated *scd1+* cells and in 61% of septated *scd1Δ* cells (Fig. 7F; Fig. S8D–F). The extent of Gef1 persistence in *scd1Δ* cells does not increase with the addition of LatA. This indicates that Scd1 is functionally epistatic to actin in the process of Gef1 removal (Fig. 7F; Fig. S8D–F). Taken together, these data suggest that Scd1 removes Gef1 from the division site after ring disassembly.

To determine the significance of Scd1-mediated removal of Gef1 from the division site, we looked at the constitutively localized *gef1S112A* mutant. Gef1S112A–3×YFP but not Gef1–3×YFP persists at the division site after ring constriction, indicated by the absence of Cdc15–tdTomato-marked actomyosin ring (Fig. S8H). Live cell imaging revealed that cell separation is delayed in *gef1S112A* mutants. Cell separation occurred 28 min after ring constriction in *gef1+* cells, but at 34 min in *gef1S112A* mutants (Fig. S8I, P=0.009). We have previously shown that prolonged Cdc42 activation at the division site impairs cell separation, as seen in other model systems (Atkins et al., 2013; Onishi et al., 2013; Wei et al., 2016). This would necessitate the removal of the GEFs from the division site. Our data indicate that Scd1-mediated Gef1 removal promotes cell separation.

DISCUSSION

While studies in yeast continue to pioneer insights into the regulation of cell polarity, one aspect of *S. pombe* polarity

Journal of Cell Science (2019) 132, jcs236018. doi:10.1242/jcs.236018

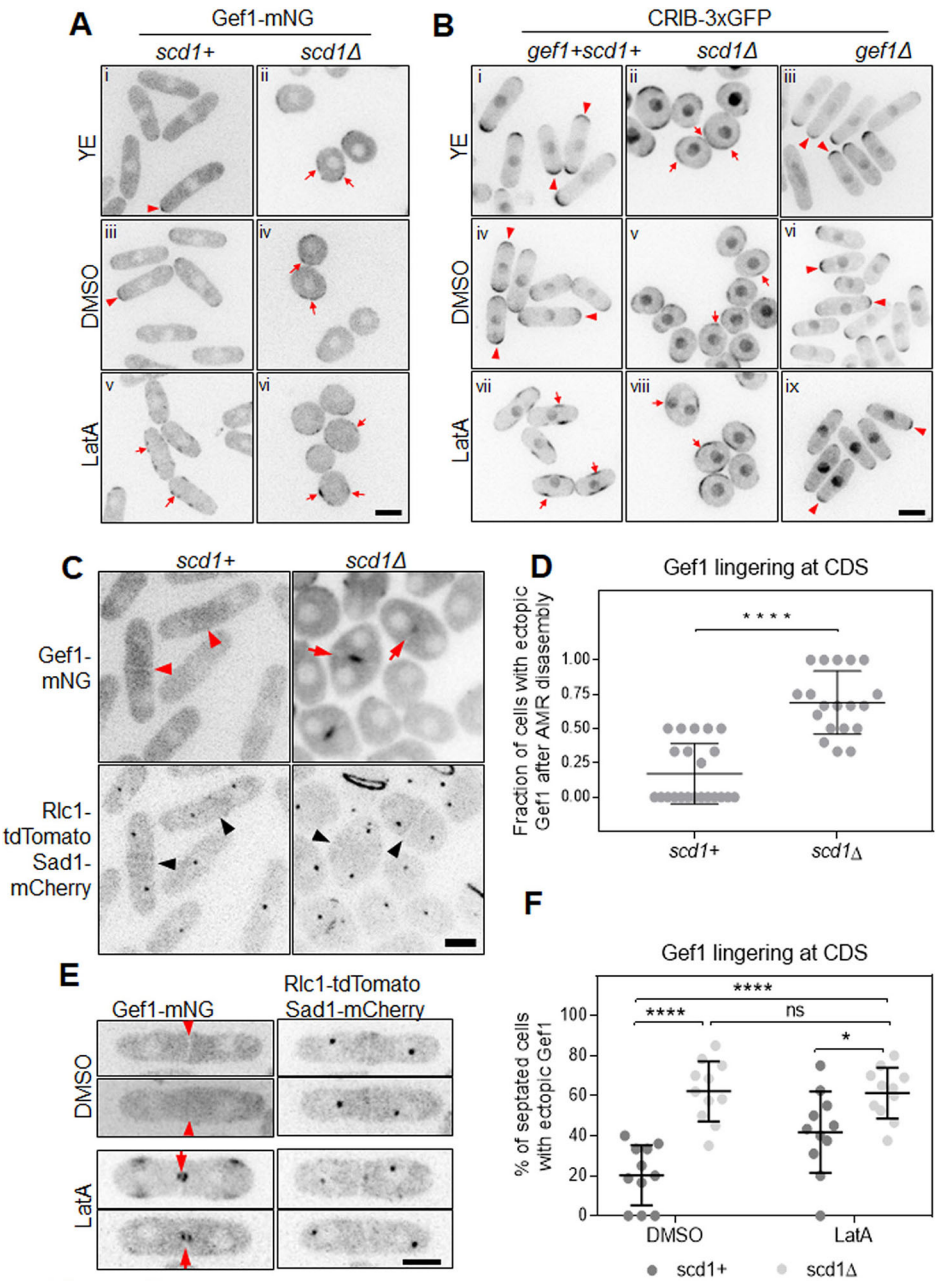

Fig. 7. Scd1 and actin prevent ectopic Gef1 localization. (A) Gef1–mNG localization in *scd1+* and *scd1Δ* cells grown in yeast extract (YE) or treated with DMSO or 10 µM LatA. (B) CRIB–3×GFP localization in *gef1+scd1+*, *scd1Δ* and *gef1Δ* cells grown in YE, or treated with DMSO or 10 µM LatA. Arrowheads, cells with Gef1–mNG or CRIB–3×GFP localized to regions of polarized growth; arrows, Gef1–mNG or CRIB–3×GFP localized to non-polarized regions on the cell cortex. (C) Gef1–mNG localization to the division site after ring disassembly in *scd1+* and *scd1Δ* cells expressing the ring and SPB markers Rlc1–tdTomato and Sad1–mCherry. Black arrowheads, division site after ring disassembly; red arrowheads, division site lacking Gef1–mNG; red arrows, Gef1–mNG localized to the division site. (D) Quantification of ectopic Gef1 lingering at the division site in *scd1+* and *scd1Δ* cells. Significance determined by Student's *t*-test; *****P*<0.0001. (E) Gef1–mNG localization in septated cells expressing the ring and SPB markers, treated with either DMSO or 10 µM LatA. Arrowheads, division site lacking Gef1–mNG; arrows, cells with Gef1–mNG localized to the membrane barrier post-ring assembly. (F) Quantification of ectopic Gef1 lingering at the division site in septated *scd1+* and *scd1Δ* cells treated with 10 µM LatA or DMSO. Significance determined by one-way ANOVA with Tukey's multiple comparisons post-hoc test; **P*<0.05. *****P*<0.0001; ns, not significant. Each data point corresponds to the mean of an analyzed field of cells (*n*>5) from the same experiment. Black bars on data points show the mean±s.d. for each genotype. All images are inverted max projections unless specified. Scale bars: 5 µm.

remains elusive: how cells initiate growth at a second site during NETO (new end take-off). We find that the Cdc42 GEF Gef1 enables the new end to overcome old end growth dominance to initiate bipolar growth. Our data indicate that Gef1 promotes the localization of the other GEF Scd1 to the new end. Uncovering the mechanism through which this occurs is not trivial, since the function of Gef1 at sites of polarized growth has proven elusive due its sparse and transient localization at these regions. Therefore, we examined the relationship between these two GEFs at the division site, where the localization of both these GEFs is easily monitored. We have previously shown that Gef1 and Scd1 localize sequentially to the division site to activate Cdc42 during cytokinesis (Wei et al., 2016). Here, we take advantage of the temporal difference between Gef1 and Scd1 localization at the division site to determine the significance of these two GEFs in Cdc42 regulation. We uncover a novel interplay between the Cdc42 GEFs that functions in both cytokinesis and polarized cell growth (Fig. 8A). Given the conserved nature of Cdc42 and its regulators, we posit that this interplay between the GEFs is a common feature of Cdc42 regulation.

Gef1-mediated Cdc42 activation promotes Scd1 recruitment via the scaffold Scd2

Analysis of Gef1-dependent Scd1 recruitment at the new end is complicated by the dynamic nature of their localization patterns, and the presence of two competing cell ends. Gef1 and Scd1 localize to the division site in a sequential manner. Moreover, during cytokinesis, the division site exclusively activates Cdc42 and thus does not compete with any other site in the cell. Therefore, we investigated Gef1 and Scd1 recruitment at the division site. We find that Scd1 localization is reduced at the division site in *gef1Δ* cells. Our observation that expression of constitutively active *cdc42G12V* can restore Scd1 localization in *gef1Δ* cells suggests that active

Journal of Cell Science (2019) 132, jcs236018. doi:10.1242/jcs.236018

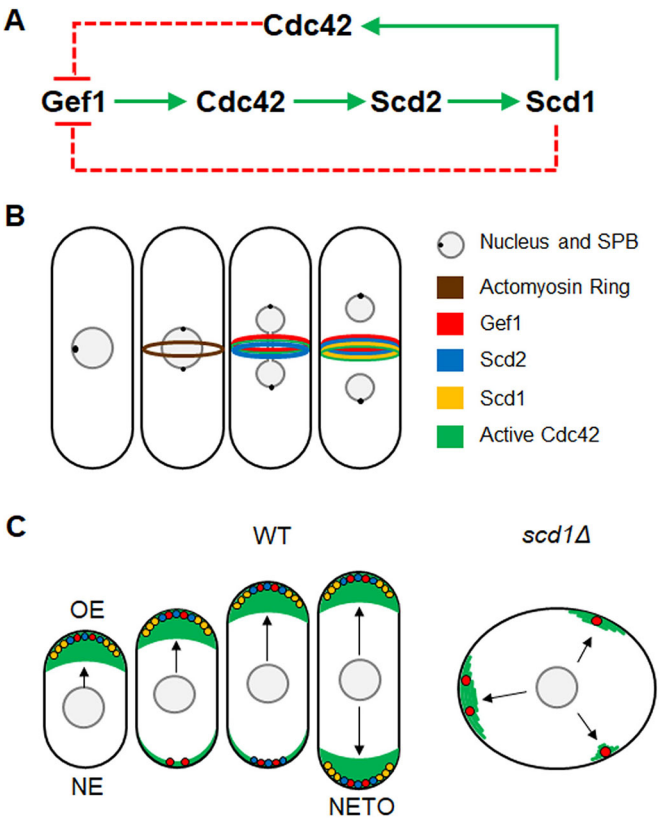

Fig. 8. Model of the crosstalk between Gef1 and Scd1 that promotes polarized bipolar growth. (A) Diagram of the crosstalk pathway between Gef1 and Scd1. Solid arrows indicate an activating or promoting relationship in the direction of the arrow. Red terminating arrow indicates inactivation or removal of the protein at the arrow terminus. Dashed arrows indicate that the mechanism that regulates the proteins to which these arrows point is not yet resolved. (B) Schematic depicting the sequential localization of Gef1, Scd2 and Scd1 to the division site during cytokinesis. At the division site, Gef1 localizes first and promotes Scd2 localization. Scd2 at the division site then recruits Scd1. (C) Schematic illustrating the crosstalk between Gef1 and Scd1 that promotes bipolar growth and regulates cell shape. In wild-type (WT) cells, Gef1 activates Cdc42, which then recruits Scd2 to the new end, leading to Scd1 recruitment and thus enabling new end take-off (NETO). In *scd1Δ* cells Gef1 localization is no longer restricted to the cell ends, leading to ectopic Cdc42 activation and loss of polarity. Arrows mark the directions of cell growth.

Cdc42 promotes Scd2 recruitment, either through direct interaction or through an alternate mechanism. A recent study indicates that Scd2 optogenetically responds to active Cdc42, and is required for Scd1-mediated positive feedback (Lamas et al., 2019, preprint). Furthermore, Scd2 interacts with GTP-Cdc42 *in vitro* (Endo et al., 2003; Wheatley and Rittinger, 2005). Similarly, the budding yeast scaffold BEM1 interacts with GTP-Cdc42 *in vivo* (Yamaguchi et al., 2007). Taken together, this suggests that Scd2 likely binds active Cdc42. Thus, we posit that Gef1 localizes to the division site first, which enables recruitment of Scd1 (Fig. 8B).

After division, the old end always initiates growth first. The two cell ends compete for active Cdc42, and initially the new end is incapable of overcoming dominance at the old end (Das et al., 2012). Gef1 promotes bipolar growth and cells lacking *gef1* are mostly monopolar (Coll et al., 2003; Das et al., 2012). In *gef1Δ* cells, new ends frequently fail to overcome old end dominance, resulting in monopolar growth. Bipolar growth in *gef1Δ* mutants is typically observed in cells that do not contain a dominant old end. We find that Cdc42 regulation at the cell ends resembles that at the division site. While Scd1 does not require Gef1 for its localization to the old end, our data suggest that Gef1 facilitates bipolar growth by promoting Scd2 localization at the new end, which is needed for Scd1 localization at this site. Polarized growth requires Cdc42 activation, mediated through positive feedback (Das and Verde, 2013; Wu and Lew, 2013). Scd1 is the positive-feedback-mediating GEF. Scd1 and Scd2 together promote a positive feedback pathway for Cdc42 activation. For such a pathway to function, Cdc42 first needs to be activated for the recruitment of Scd2, and consequently Scd1. Our data indicate that Gef1-mediated Cdc42 activation provides the seed for Scd1–Scd2 recruitment. This enables Scd2 recruitment to nascent sites that have no prior history of Cdc42 activation and enables Scd1 recruitment to those sites. Thus, Gef1 activates Cdc42 to establish a Scd1-dependent positive feedback pathway at the new end to overcome old end dominance and establish bipolar growth (Fig. 8C). A recent report indicates that Gef1 localization to the division site and to the sites of polarized cell growth depends on the F-BAR protein Cdc15 (Hercyk and Das, 2019). This provides further evidence that while the division site and cell ends are functionally distinct, some aspects of Cdc42 regulation are conserved at these sites.

Scd1 prevents ectopic Gef1 localization

Scd1 is the primary GEF that promotes polarized growth (Chang et al., 1994). We find that cells lacking *scd1* are depolarized due to ectopic Cdc42 activation, as a result of mislocalized Gef1. In the presence of Scd1, Gef1 shows sparse cortical localization and is restricted to the cell ends. Cell ends that do not localize Scd1 either due to LatA treatment or *scd1* knockdown display ectopic and enhanced cortical localization of Gef1. Thus, we posit that Scd1 prevents ectopic Gef1 localization. A recent report shows that ectopic Cdc42 activation in LatA-treated cells depends on the stress-activated MAP kinase Sty1 (Mutavchiev et al., 2016). Cells treated with LatA did not display ectopic Cdc42 activation in the absence of *sty1*. It is possible that in the absence of actin, reduced Scd1 at the cell cortex elicits a stress response, leading to Sty1 activation that results in the mislocalization of Gef1. Further analysis is necessary to test this hypothesis.

Normally, Gef1 localization to the division site is lost after ring constriction (Wei et al., 2016). Similar to our observation at the cell cortex, we find that Gef1 persists at the division site in cells lacking Scd1 or in cells treated with LatA. Here, we show that Scd1 promotes the clearance of Gef1 from the division site after ring disassembly (Fig. 8A). Failure to inactivate Cdc42 results in cytokinesis failure in budding yeast and HeLa cells, and prevents cellularization in *Drosophila* embryos (Atkins et al., 2013; Crawford et al., 1998; Dutartre et al., 1996; Onishi et al., 2013). Our data suggest that Scd1 ensures Gef1 removal from the division site in the final stages of cytokinesis, preventing inappropriate Cdc42 activation. Taken together, our data demonstrate an elegant regulatory pattern in which Gef1-mediated Scd1 recruitment to the division site promotes septum formation, and Scd1-mediated Gef1 removal promotes cell separation.

Multiple GEFs combinatorially regulate Cdc42 during complex processes

Polarized cell growth requires symmetry breaking, and several models have indicated a need for Cdc42 positive feedback loops in this process (Bendezú et al., 2015; Irazoqui et al., 2003; Kozubowski et al., 2008; Slaughter et al., 2009a,b; Wedlich-Soldner et al., 2004). Elegant experiments in budding yeast demonstrate that local activation of Cdc42 establishes positive feedback through the

Journal of Cell Science (2019) 132, jcs236018. doi:10.1242/jcs.236018

recruitment of additional GEFs to amplify the conversion of GDP-Cdc42 to GTP-Cdc42 (Butty et al., 2002; Kozubowski et al., 2008). A caveat of positive feedback is that the site that first activates Cdc42 can act as a sink that traps the GEFs, thereby preventing Cdc42 activation at other sites. Such a trap can be undone via negative feedback regulation of Cdc42 that results in an oscillatory pattern at the cell ends (Das et al., 2012; Howell et al., 2012). Negative feedback in *S. pombe* and *S. cerevisiae* acts through Pak1 kinase activity that antagonizes either the Cdc42 scaffold or the GEF (Das et al., 2012; Gulli et al., 2000; Kuo et al., 2014; Rapali et al., 2017). Indeed, *pak1* mutants fail to activate bipolar growth (Das et al., 2012; Verde et al., 1998). Although fission yeast contains another Pak homolog, Shk2, only Pak1 (Shk1) is essential. Furthermore, Shk2 functions primarily during G0 and meiosis, and its loss does not result in the same polarity defects as loss of Pak1 (Vještica et al., 2018; Yang et al., 1998). Importantly, Shk2 binds neither Scd1 nor Scd2 (Sells et al., 1998; Yang et al., 1998). Therefore, it is unlikely that Shk2 mediates Scd1 localization and further investigations will test this. Our data show that besides the kinase Pak1, Gef1 also contributes to initiation of bipolar growth.

The Cdc42 oscillatory pattern can be explained by the presence of positive feedback, time-delayed negative feedback, and competition between the two ends for active Cdc42. We posit that Scd1 activates Cdc42 through positive feedback at the dominant old end. Dominance at the old end ensures that Scd1 localization is mainly restricted to this end at the expense of the new end. A previous model suggests that as the cell reaches a certain size, the GEFs reach a threshold level that allows the new end to overcome old end dominance to initiate growth and promote bipolarity (Das et al., 2012). Threshold GEF levels alone cannot explain our findings since *gef1S112A* cells display bipolar growth at a smaller cell size (Das et al., 2015), while G1-arrested *cdc10-129* mutants grow to longer cell lengths but remain monopolar. Our data suggest that the regulatory crosstalk between the Cdc42 GEFs may provide an advantage to the cell and enable the new end to overcome old end dominance. Gef1 triggers a positive feedback at the division site via a feed-forward pathway (Fig. 8A,C). Given that Gef1 promotes Scd1-mediated polarized growth at the new end, it is conceivable that Gef1 itself is tightly regulated to prevent random Cdc42 activation. Indeed, Gef1 shows sparse localization to the cell ends and is mainly cytoplasmic (Das et al., 2015). The NDR kinase Orb6 prevents ectopic Gef1 localization via the 14-3-3 protein Rad24-mediated sequestration to the cytoplasm (Das et al., 2015, 2009). Here, we show that while Gef1 promotes Scd1 recruitment to a nascent site, Scd1 itself restricts Gef1 localization to the cell ends to precisely activate Cdc42 (Fig. 8C). Taken together, our findings describe an elegant system in which the two Cdc42 GEFs regulate each other to ensure proper cell polarization.

Significance of GEF coordination in other systems

In budding yeast, CDC24 is required for polarization during bud emergence and is essential for viability (Sloat et al., 1981; Sloat and Pringle, 1978), unlike Scd1 in fission yeast. Budding yeast also has a second GEF, BUD3, which establishes a proper bud site (Kang et al., 2014). During G1 in budding yeast, bud emergence occurs via biphasic CDC42 activation by the two GEFs: BUD3 helps select the bud site (Kang et al., 2014), and CDC24 allows polarization (Sloat et al., 1981; Sloat and Pringle, 1978). This is analogous to new end growth in fission yeast, which requires Gef1-dependent recruitment of Scd1 for robust Cdc42 activation. It would be interesting to test whether crosstalk also exists between BUD3 and CDC24 in budding yeast.

The Rho family of GTPases includes Rho, Rac and Cdc42. In certain mammalian cells, Cdc42 and Rac1 appear to activate cell growth in a biphasic manner (de Beco et al., 2018; Yang et al., 2016). For example, during motility, the GTPases, Rho, Rac and Cdc42, regulate the actin cytoskeleton (Heasman and Ridley, 2008; Machacek et al., 2009). During cell migration, these GTPases form bands or 'zones' in the leading and trailing regions of the cell (Ridley, 2015). Their spatial separation is mediated by the organization of their GEFs and GAPs, and by regulatory signaling between these GTPases (Guilluy et al., 2011). Cdc42 and Rho are mutually antagonistic, explaining how such zones of GTPase activity can be established and maintained (Guilluy et al., 2011; Kutys and Yamada, 2014; Warner and Longmore, 2009). Similarly, Cdc42 can refine Rac activity (Guilluy et al., 2011). Recent experiments demonstrate that during cell migration, reorganization of the actin cytoskeleton occurs in a biphasic manner, in which Cdc42 activation at new sites sets the direction, while robust Rac activation determines the speed (de Beco et al., 2018; Yang et al., 2016). Unlike most eukaryotes, the genome of *S. pombe* does not contain a Rac GTPase. However, the GEFs differentially activate Cdc42, such that Gef1 sets the direction of growth by establishing a new site of polarization, while Scd1 promotes efficient growth through robust Cdc42 activation. In conclusion, we propose that the crosstalk between the Cdc42 GEFs themselves is an intrinsic property of small GTPases and is necessary for fine-tuning their activity.

MATERIALS AND METHODS

Strains and cell culture

The *S. pombe* strains used in this study are listed in Table S1. All strains are isogenic to the original strain PN567. Cells were cultured in yeast extract (YE) medium and grown exponentially at 25°C, unless specified otherwise. Standard techniques were used for genetic manipulation and analysis (Moreno et al., 1991). Cells were grown exponentially for at least three rounds of eight generations each before imaging.

Microscopy

Cells were imaged at room temperature (23–25°C) with an Olympus IX83 microscope equipped with a VTHawk two-dimensional array laser scanning confocal microscopy system (Visitech International, Sunderland, UK), electron-multiplying charge-coupled device digital camera (Hamamatsu, Hamamatsu City, Japan), and 100×/numerical aperture 1.49 UAPO lens (Olympus, Tokyo, Japan). Images were acquired with MetaMorph (Molecular Devices, Sunnyvale, CA) and analyzed using ImageJ (National Institutes of Health, Bethesda, MD).

Analysis of growth pattern

The growth pattern of *gef1+* and *gef1Δ* cells was observed by live imaging of cells through multiple generations. Cells were placed in 3.5-mm glass-bottom culture dishes (MatTek, Ashland, MA) and overlaid with YE medium plus 1% agar, and 100 µM ascorbic acid to minimize photo-toxicity to the cell. A bright-field image was acquired every minute for 12 h. Birth scars were used to distinguish between, and to measure, old end and new end growth.

Construction of fluorescently tagged Gef1 fusion proteins

The forward primer 5′-GGATCCGTGTTTACCAAAGTTATGTAAGAC-3′ with a 5′ BamHI site and the reverse primer 5′-CCCGGGAACCCTC-GCAGCTAAAGA-3′ with a 5′ XmaI site were used to amplify a 3 kb DNA fragment containing *gef1*, the 5′ UTR, and the endogenous promoter. The fragment was then digested with SalI and XmaI and ligated into the SalI-XmaI site of pKS392 pFA6-tdTomato-kanMX and pKG6507 pFA6-mNeonGreen-kanMX. Constructs were linearized by digestion with XbaI and transformed into the *gef1* locus in wild-type cells.

Expression of constitutively active Cdc42

pjk148-nmt41x-leu1^{+} or *pjk148-nmt41x:cdc42G12V-leu1*$^{+}$ were linearized with NdeI and integrated into the *leu1-32* locus in *gef1+* and *gef1Δ* cells

expressing either CRIB–3×GFP and Scd1–tdTomato, or Scd1–tdTomato and Rlc1–GFP. The empty vector *pjk148-nmt41x-leu1*$^{+}$ was used as control. Cells were grown in EMM with 0.05 µM thiamine to promote minimal expression of *cdc42G12V*.

Calcofluor staining

To visualize areas of cell growth, cells were stained in YE liquid with 50 µg/ml Calcofluor White M2R (Sigma-Aldrich, St Louis, MO) at room temperature.

Latrunculin A treatment

Cells in YE were incubated at room temperature with 10 µM or 100 µM latrunculin A (Millipore-Sigma) dissolved in dimethyl sulfoxide (DMSO) for 40 min prior to imaging. Control cells were treated with 1% DMSO and incubated for 40 min.

Analysis of fluorescence intensity

Mutants expressing fluorescent proteins were grown to OD 0.5 and imaged on slides. Cells in slides were imaged for no more than 3 min to prevent any stress response as previously described (Das et al., 2015). Depending on the mutant and the fluorophore, 16–28 *z*-planes were collected at a *z*-interval of 0.4 µm for either or both the 488 nm and 561 nm channels. The respective controls were grown and imaged in an identical manner. ImageJ was used to generate sum projections from the *z*-series, and to measure the fluorescence intensity of a selected region (actomyosin ring, or growth cap at cell tip). The background fluorescence in a cell-free region of the image was subtracted to generate the normalized intensity. Mean normalized intensity was calculated for each image from all (n>5) measurable cells within each field. A Student's two-tailed *t*-test, assuming unequal variance, was used to determine significance through comparison of each strain's mean normalized intensities.

Statistical tests

GraphPad Prism was used to determine significance. One-way ANOVA, followed by a Tukey's multiple comparisons post-hoc test, was used to determine individual *P*-values when comparing three or more samples. When comparing two samples, a Student's *t*-test (two-tailed, unequal variance) was used to determine significance.

Acknowledgements

We thank Joshua Bembenek and Tessa Burch-Smith for critical review of our manuscript; Kathy Gould (Vanderbilt University, Nashville, USA) for supplying plasmids; and Mohan Balasubramanian (University of Warwick, Coventry, UK) and Sophie Martin (University of Lausanne, Switzerland) for providing strains.

Competing interests

The authors declare no competing or financial interests.

Author contributions

Conceptualization: B.S.H., M.E.D.; Validation: B.S.H.; Formal analysis: B.S.H., J.R.-R., A.S.M., M.A.H.; Investigation: B.S.H., J.R.-R., A.S.M., M.A.H.; Resources: M.E.D.; Writing - original draft: B.S.H.; Writing - review & editing: B.S.H., J.R.-R., M.E.D.; Supervision: M.E.D.; Project administration: M.E.D.; Funding acquisition: M.E.D.

Funding

This work was supported by a grant from the National Science Foundation (1616495). J.R.-R. was supported by National Institutes of Health IMSD (R25GM086761) and is currently supported by a National Science Foundation GRFP (1452154). Deposited in PMC for release after 12 months.

Supplementary information

Supplementary information available online at
http://jcs.biologists.org/lookup/doi/10.1242/jcs.236018.supplemental

References

Atkins, B. D., Yoshida, S., Saito, K., Wu, C. F., Lew, D. J. and Pellman, D. (2013). Inhibition of Cdc42 during mitotic exit is required for cytokinesis. *J. Cell Biol.* **202**, 231-240. doi:10.1083/jcb.201301090

Bendezú, F. O. and Martin, S. G. (2013). Cdc42 explores the cell periphery for mate selection in fission yeast. *Curr. Biol.* **23**, 42-47. doi:10.1016/j.cub.2012.10.042

Bendezú, F. O., Vincenzetti, V., Vavylonis, D., Wyss, R., Vogel, H. and Martin, S. G. (2015). Spontaneous Cdc42 polarization independent of GDI-mediated extraction and actin-based trafficking. *PLoS Biol.* **13**, e1002097. doi:10.1371/journal.pbio.1002097

Bos, J. L., Rehmann, H. and Wittinghofer, A. (2007). GEFs and GAPs: critical elements in the control of small G proteins. *Cell* **129**, 865-877. doi:10.1016/j.cell.2007.05.018

Butty, A.-C., Perrinjaquet, N., Petit, A., Jaquenoud, M., Segall, J. E., Hofmann, K., Zwahlen, C. and Peter, M. (2002). A positive feedback loop stabilizes the guanine-nucleotide exchange factor Cdc24 at sites of polarization. *EMBO J.* **21**, 1565-1576. doi:10.1093/emboj/21.7.1565

Chang, E. C., Barr, M., Wang, Y., Jung, V., Xu, H.-P. and Wigler, M. H. (1994). Cooperative interaction of S. pombe proteins required for mating and morphogenesis. *Cell* **79**, 131-141. doi:10.1016/0092-8674(94)90406-5

Coll, P. M., Trillo, Y., Ametzazurra, A. and Perez, P. (2003). Gef1p, a new guanine nucleotide exchange factor for Cdc42p, regulates polarity in Schizosaccharomyces pombe. *Mol. Biol. Cell* **14**, 313-323. doi:10.1091/mbc.e02-07-0400

Crawford, J. M., Harden, N., Leung, T., Lim, L. and Kiehart, D. P. (1998). Cellularization in Drosophila melanogaster is disrupted by the inhibition of rho activity and the activation of Cdc42 function. *Dev. Biol.* **204**, 151-164. doi:10.1006/dbio.1998.9061

Das, M. and Verde, F. (2013). Role of Cdc42 dynamics in the control of fission yeast cell polarization. *Biochem. Soc. Trans.* **41**, 1745-1749. doi:10.1042/BST20130241

Das, M., Wiley, D. J., Chen, X., Shah, K. and Verde, F. (2009). The conserved NDR kinase Orb6 controls polarized cell growth by spatial regulation of the small GTPase Cdc42. *Curr. Biol.* **19**, 1314-1319. doi:10.1016/j.cub.2009.06.057

Das, M., Drake, T., Wiley, D. J., Buchwald, P., Vavylonis, D. and Verde, F. (2012). Oscillatory dynamics of Cdc42 GTPase in the control of polarized growth. *Science* **337**, 239-243. doi:10.1126/science.1218377

Das, M., Nunez, I., Rodriguez, M., Wiley, D. J., Rodriguez, J., Sarkeshik, A., Yates, J. R., III, Buchwald, P. and Verde, F. (2015). Phosphorylation-dependent inhibition of Cdc42 GEF Gef1 by 14-3-3 protein Rad24 spatially regulates Cdc42 GTPase activity and oscillatory dynamics during cell morphogenesis. *Mol. Biol. Cell* **26**, 3373-3556. doi:10.1091/mbc.E15-02-0095

de Beco, S., Vaidziulyte, K., Manzi, J., Dalier, F., di Federico, F., Cornilleau, G., Dahan, M. and Coppey, M. (2018). Optogenetic dissection of Rac1 and Cdc42 gradient shaping. *Nat. Commun.* **9**, 4816. doi:10.1038/s41467-018-07286-8

Drubin, D. G. and Nelson, W. J. (1996). Origins of cell polarity. *Cell* **84**, 335-344. doi:10.1016/S0092-8674(00)81278-7

Dutartre, H., Davoust, J., Gorvel, J. P. and Chavrier, P. (1996). Cytokinesis arrest and redistribution of actin-cytoskeleton regulatory components in cells expressing the Rho GTPase CDC42Hs. *J. Cell Sci.* **109**, 367-377.

Endo, M., Shirouzu, M. and Yokoyama, S. (2003). The Cdc42 binding and scaffolding activities of the fission yeast adaptor protein Scd2. *J. Biol. Chem.* **278**, 843-852. doi:10.1074/jbc.M209714200

Estravís, M., Rincon, S. A., Santos, B. and Pérez, P. (2011). Cdc42 regulates multiple membrane traffic events in fission yeast. *Traffic* **12**, 1744-1758. doi:10.1111/j.1600-0854.2011.01275.x

Estravís, M., Rincon, S. and Pérez, P. (2012). Cdc42 regulation of polarized traffic in fission yeast. *Commun. Integr. Biol.* **5**, 370-373. doi:10.4161/cib.19977

Etienne-Manneville, S. (2004). Cdc42–the centre of polarity. *J. Cell Sci.* **117**, 1291-1300. doi:10.1242/jcs.01115

Guilluy, C., Garcia-Mata, R. and Burridge, K. (2011). Rho protein crosstalk: another social network? *Trends Cell Biol.* **21**, 718-726. doi:10.1016/j.tcb.2011.08.002

Gulli, M. P., Jaquenoud, M., Shimada, Y., Niederhauser, G., Wiget, P. and Peter, M. (2000). Phosphorylation of the Cdc42 exchange factor Cdc24 by the PAK-like kinase Cla4 may regulate polarized growth in yeast. *Mol. Cell* **6**, 1155-1167. doi:10.1016/S1097-2765(00)00113-1

Harris, K. P. and Tepass, U. (2010). Cdc42 and vesicle trafficking in polarized cells. *Traffic* **11**, 1272-1279. doi:10.1111/j.1600-0854.2010.01102.x

Heasman, S. J. and Ridley, A. J. (2008). Mammalian Rho GTPases: new insights into their functions from in vivo studies. *Nat. Rev. Mol. Cell Biol.* **9**, 690-701. doi:10.1038/nrm2476

Hercyk, B. S. and Das, M. E. (2019). F-BAR Cdc15 promotes Gef1-mediated Cdc42 activation during cytokinesis and cell polarization in S. pombe. *Genetics* doi:10.1534/genetics.119.302649. doi:10.1534/genetics.119.302649

Howell, A. S., Jin, M., Wu, C.-F., Zyla, T. R., Elston, T. C. and Lew, D. J. (2012). Negative feedback enhances robustness in the yeast polarity establishment circuit. *Cell* **149**, 322-333. doi:10.1016/j.cell.2012.03.012

Irazoqui, J. E., Gladfelter, A. S. and Lew, D. J. (2003). Scaffold-mediated symmetry breaking by Cdc42p. *Nat. Cell Biol.* **5**, 1062-1070. doi:10.1038/ncb1068

Johnson, D. I. (1999). Cdc42: an essential Rho-type GTPase controlling eukaryotic cell polarity. *Microbiol. Mol. Biol. Rev.* **63**, 54-105.

Kang, P. J., Lee, M. E. and Park, H. O. (2014). Bud3 activates Cdc42 to establish a proper growth site in budding yeast. *J. Cell Biol.* **206**, 19-28. doi:10.1083/jcb.201402040

Kelly, F. D. and Nurse, P. (2011). Spatial control of Cdc42 activation determines cell width in fission yeast. *Mol. Biol. Cell* **22**, 3801-3811. doi:10.1091/mbc.e11-01-0057

Kozubowski, L., Saito, K., Johnson, J. M., Howell, A. S., Zyla, T. R. and Lew, D. J. (2008). Symmetry-breaking polarization driven by a Cdc42p GEF-PAK complex. *Curr. Biol.* **18**, 1719-1726. doi:10.1016/j.cub.2008.09.060

Kuo, C.-C., Savage, N. S., Chen, H., Wu, C. F., Zyla, T. R. and Lew, D. J. (2014). Inhibitory GEF phosphorylation provides negative feedback in the yeast polarity circuit. *Curr. Biol.* **24**, 753-759. doi:10.1016/j.cub.2014.02.024

Kutys, M. L. and Yamada, K. M. (2014). An extracellular-matrix-specific GEF-GAP interaction regulates Rho GTPase crosstalk for 3D collagen migration. *Nat. Cell Biol.* **16**, 909-917. doi:10.1038/ncb3026

Lamas, I., Merlini, L., Vještica, A., Vincenzetti, V. and Martin, S. G. (2019). Optogenetics reveals Cdc42 local activation by scaffold-mediated positive feedback and Ras GTPase. *bioRxiv* 710855. doi:10.1101/710855

Machacek, M., Hodgson, L., Welch, C., Elliott, H., Pertz, O., Nalbant, P., Abell, A., Johnson, G. L., Hahn, K. M. and Danuser, G. (2009). Coordination of Rho GTPase activities during cell protrusion. *Nature* **461**, 99-103. doi:10.1038/nature08242

Marks, J., Hagan, I. M. and Hyams, J. S. (1986). Growth polarity and cytokinesis in fission yeast: the role of the cytoskeleton. *J. Cell Sci.* **1986**, Suppl 5, 229-241. doi:10.1242/jcs.1986.Supplement_5.15

Mitchison, J. M. and Nurse, P. (1985). Growth in cell length in the fission yeast Schizosaccharomyces pombe. *J. Cell Sci.* **75**, 357-376.

Moreno, S., Klar, A. and Nurse, P. (1991). Molecular genetic analysis of fission yeast Schizosaccharomyces pombe. *Methods Enzymol.* **194**, 795-823. doi:10.1016/0076-6879(91)94059-L

Mutavchiev, D. R., Leda, M. and Sawin, K. E. (2016). Remodeling of the fission yeast Cdc42 cell-polarity module via the Sty1 p38 stress-activated protein kinase pathway. *Curr. Biol.* **26**, 2921-2928. doi:10.1016/j.cub.2016.08.048

Nabeshima, K., Nakagawa, T., Straight, A. F., Murray, A., Chikashige, Y., Yamashita, Y. M., Hiraoka, Y. and Yanagida, M. (1998). Dynamics of centromeres during metaphase-anaphase transition in fission yeast: Dis1 is implicated in force balance in metaphase bipolar spindle. *Mol. Biol. Cell* **9**, 3211-3225. doi:10.1091/mbc.9.11.3211

Nance, J. and Zallen, J. A. (2011). Elaborating polarity: PAR proteins and the cytoskeleton. *Development* **138**, 799-809. doi:10.1242/dev.053538

Onishi, M., Ko, N., Nishihama, R. and Pringle, J. R. (2013). Distinct roles of Rho1, Cdc42, and Cyk3 in septum formation and abscission during yeast cytokinesis. *J. Cell Biol.* **202**, 311-329. doi:10.1083/jcb.201302001

Rapali, P., Mitteau, R., Braun, C., Massoni-Laporte, A., Ünlu, C., Bataille, L., Arramon, F. S., Gygi, S. P. and McCusker, D. (2017). Scaffold-mediated gating of Cdc42 signalling flux. *eLife* **6**, 231. doi:10.7554/eLife.25257

Ridley, A. J. (2006). Rho GTPases and actin dynamics in membrane protrusions and vesicle trafficking. *Trends Cell Biol.* **16**, 522-529. doi:10.1016/j.tcb.2006.08.006

Ridley, A. J. (2015). Rho GTPase signalling in cell migration. *Curr. Opin. Cell Biol.* **36**, 103-112. doi:10.1016/j.ceb.2015.08.005

Sells, M. A., Barratt, J. T., Caviston, J., Ottilie, S., Leberer, E. and Chernoff, J. (1998). Characterization of Pak2p, a pleckstrin homology domain-containing, p21-activated protein kinase from fission yeast. *J. Biol. Chem.* **273**, 18490-18498. doi:10.1074/jbc.273.29.18490

Slaughter, B. D., Das, A., Schwartz, J. W., Rubinstein, B. and Li, R. (2009a). Dual modes of cdc42 recycling fine-tune polarized morphogenesis. *Dev. Cell* **17**, 823-835. doi:10.1016/j.devcel.2009.10.022

Slaughter, B. D., Smith, S. E. and Li, R. (2009b). Symmetry breaking in the life cycle of the budding yeast. *Cold Spring Harbor Perspect. Biol.* **1**, a003384. doi:10.1101/cshperspect.a003384

Sloat, B. F. and Pringle, J. R. (1978). A mutant of yeast defective in cellular morphogenesis. *Science* **200**, 1171-1173. doi:10.1126/science.349694

Sloat, B. F., Adams, A. and Pringle, J. R. (1981). Roles of the CDC24 gene product in cellular morphogenesis during the Saccharomyces cerevisiae cell cycle. *J. Cell Biol.* **89**, 395-405. doi:10.1083/jcb.89.3.395

Tay, Y. D., Leda, M., Goryachev, A. B. and Sawin, K. E. (2018). Local and global Cdc42 guanine nucleotide exchange factors for fission yeast cell polarity are coordinated by microtubules and the Tea1-Tea4-Pom1 axis. *J. Cell Sci.* **131**, jcs216580. doi:10.1242/jcs.216580

Verde, F., Wiley, D. J. and Nurse, P. (1998). Fission yeast orb6, a ser/thr protein kinase related to mammalian rho kinase and myotonic dystrophy kinase, is required for maintenance of cell polarity and coordinates cell morphogenesis with the cell cycle. *Proc. Natl. Acad. Sci. USA* **95**, 7526-7531. doi:10.1073/pnas.95.13.7526

Vještica, A., Merlini, L., Nkosi, P. J. and Martin, S. G. (2018). Gamete fusion triggers bipartite transcription factor assembly to block re-fertilization. *Nature* **560**, 397-400. doi:10.1038/s41586-018-0407-5

Warner, S. J. and Longmore, G. D. (2009). Cdc42 antagonizes Rho1 activity at adherens junctions to limit epithelial cell apical tension. *J. Cell Biol.* **187**, 119-133. doi:10.1083/jcb.200906047

Wedlich-Soldner, R., Wai, S. C., Schmidt, T. and Li, R. (2004). Robust cell polarity is a dynamic state established by coupling transport and GTPase signaling. *J. Cell Biol.* **166**, 889-900. doi:10.1083/jcb.200405061

Wei, B., Hercyk, B. S., Mattson, N., Mohammadi, A., Rich, J., DeBruyne, E., Clark, M. M. and Das, M. (2016). Unique spatiotemporal activation pattern of Cdc42 by Gef1 and Scd1 promotes different events during Cytokinesis. *Mol. Biol. Cell* **27**, 1235-1245. doi:10.1091/mbc.E15-10-0700

Wheatley, E. and Rittinger, K. (2005). Interactions between Cdc42 and the scaffold protein Scd2: requirement of SH3 domains for GTPase binding. *Biochem. J.* **388**, 177-184. doi:10.1042/BJ20041838

Witte, K., Strickland, D. and Glotzer, M. (2017). Cell cycle entry triggers a switch between two modes of Cdc42 activation during yeast polarization. *eLife* **6**, 231. doi:10.7554/eLife.26722

Wu, C.-F. and Lew, D. J. (2013). Beyond symmetry-breaking: competition and negative feedback in GTPase regulation. *Trends Cell Biol.* **23**, 476-483. doi:10.1016/j.tcb.2013.05.003

Wu, J. Q., Kuhn, J. R., Kovar, D. R. and Pollard, T. D. (2003). Spatial and temporal pathway for assembly and constriction of the contractile ring in fission yeast cytokinesis. *Dev. Cell* **5**, 723-734. doi:10.1016/S1534-5807(03)00324-1

Yamaguchi, Y., Ota, K. and Ito, T. (2007). A novel Cdc42-interacting domain of the yeast polarity establishment protein Bem1. Implications for modulation of mating pheromone signaling. *J. Biol. Chem.* **282**, 29-38. doi:10.1074/jbc.M609308200

Yang, P., Kansra, S., Pimental, R. A., Gilbreth, M. and Marcus, S. (1998). Cloning and characterization of shk2, a gene encoding a novel p21-activated protein kinase from fission yeast. *J. Biol. Chem.* **273**, 18481-18489. doi:10.1074/jbc.273.29.18481

Yang, H. W., Collins, S. R. and Meyer, T. (2016). Locally excitable Cdc42 signals steer cells during chemotaxis. *Nat. Cell Biol.* **18**, 191-201. doi:10.1038/ncb3292

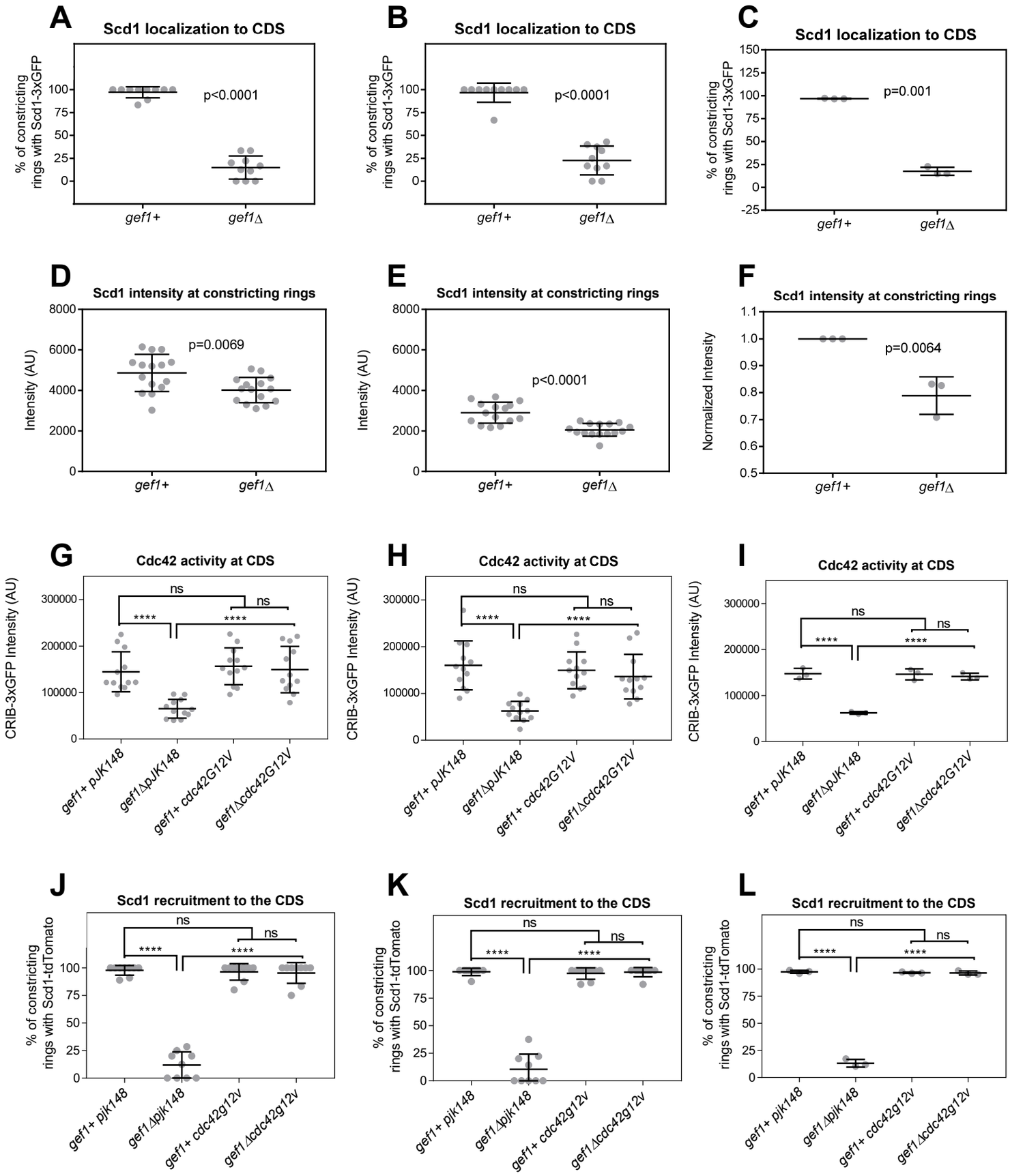

Supplemental Figure 1

Figure S1: (A-F) Gef1 mediates Scd1 localization to the division site. (A and B) Quantification of 2 additional independent replicates of the experiment depicted in Fig. 1A,B. **(C)** Quantification of the means from all 3 replicate experiments. **(D and E)** Quantification of 2 additional independent replicates of the experiment depicted in Fig. 1A,C. **(F)** Quantification of the means from all 3 replicate experiments. All data points are plotted in each graph, with black bars on top of data points that show the mean and standard deviation for each genotype. Each data point corresponds to the mean of an analyzed field of cells (n>5) from the same experiment. Reported p values from Student's t-tests. **(G-L) Gef1-mediated Cdc42 activation recruits Scd1 to the division site. (G and H)** Quantification of 2 additional independent replicates of the experiment depicted in Fig. 1D,E. **(I)** Quantification of the means from all 3 replicate experiments. **(J and K)** Quantification of 2 additional independent replicates of the experiment depicted in Fig. 1,F,G. **(L)** Quantification of the means from all 3 replicate experiments. All data points are plotted in each graph, with black bars on top of data points that show the mean and standard deviation for each genotype. Each data point corresponds to the mean of an analyzed field of cells (n>5) from the same experiment. Significance determined by one-way ANOVA with Tukey's multiple comparisons post hoc test (****, $p<0.0001$, ns, not significant).

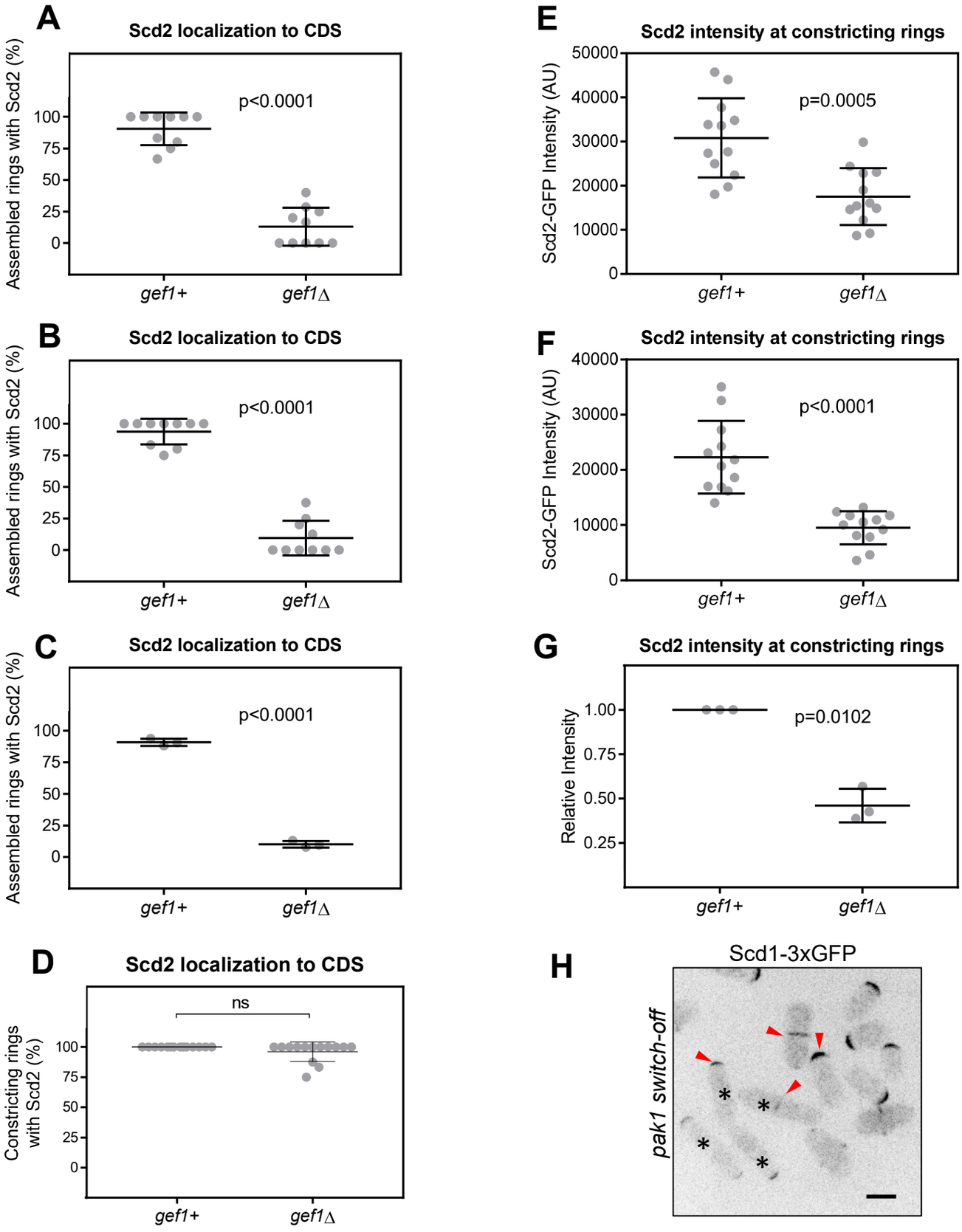

Supplemental Figure 2

Figure S2: (A-G) Gef1 promotes Scd2 localization to the division site. (A and B) Quantification of 2 additional independent replicates of the experiment depicted in Fig. 2A,B. **(C)** Quantification of the means from all 3 replicate experiments. **(D) Scd2 localization to the division site is delayed until the onset of ring constriction in *gef1Δ*.** Quantification of Scd2-GFP localization to constricting rings in *gef1+* and *gef1Δ*. (ns, not significant). **(E and F)** Quantification of 2 additional independent replicates of the experiment depicted in Fig. 2A,C. **(G)** Quantification of the means from all 3 replicate experiments. All data points are plotted in each graph, with black bars on top of data points that show the mean and standard deviation for each genotype. Each data point corresponds to the mean of an analyzed field of cells (n>5) from the same experiment. Reported p values from Student's t-tests. **(H) The PAK kinase antagonizes Scd1 accumulation to limit Cdc42 activity.** Scd1-3xGFP accumulation in *pak1+* and nmt1:*pak1 switch-off* mutant cells. Cells were grown to an OD of 0.5 in minimal media + thiamine and mixed prior to imaging. Red arrow heads mark the site of Scd1-3xGFP localization and asterisks indicate *pak1+* cells. Images are inverted max projections.

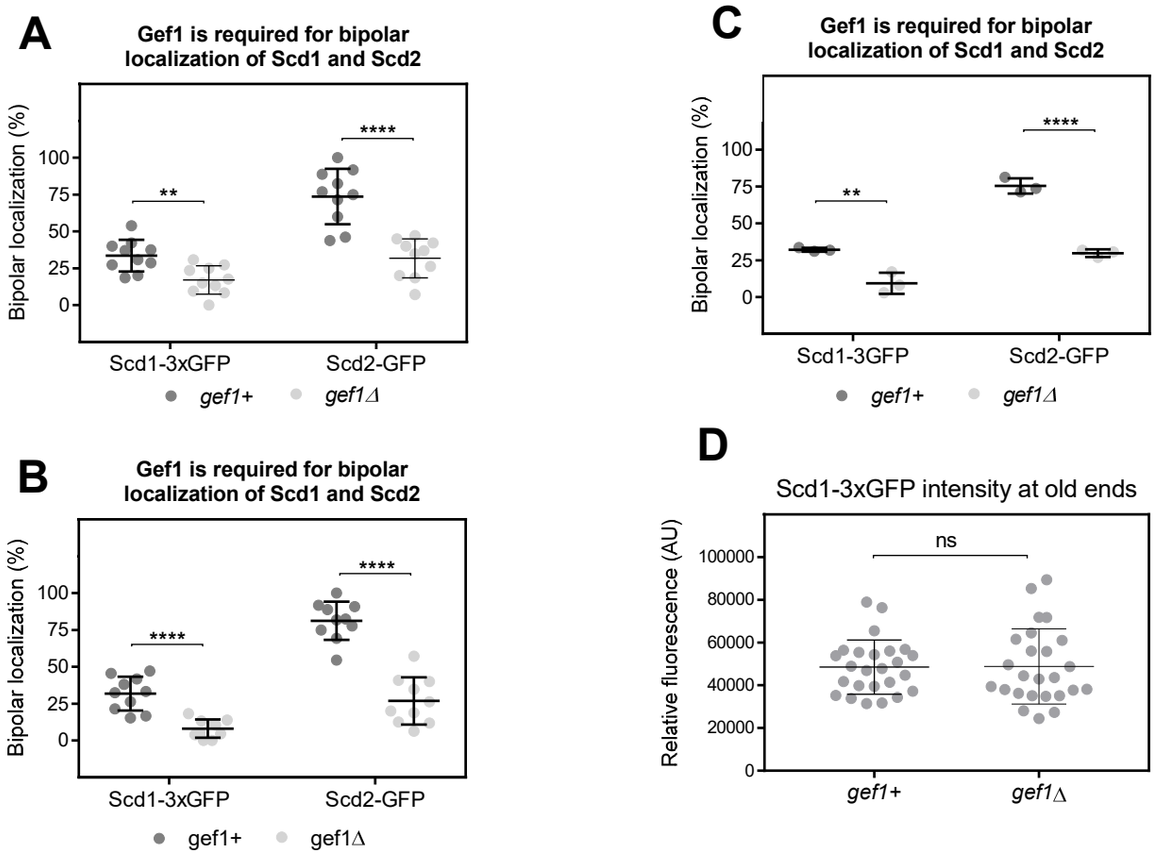

Figure S3: (A-C) Gef1 mediates bipolar localization of Scd1 and Scd2. (A and B) Quantification of 2 additional independent replicates of the experiment depicted in Fig. 4A,B. **(C)** Quantification of the means from all 3 replicate experiments. All data points are plotted in each graph, with black bars on top of data points that show the mean and standard deviation for each genotype. Each data point corresponds to the mean of an analyzed field of cells (n>5) from the same experiment. Significance determined by one-way ANOVA with Tukey's multiple comparisons post hoc test (****, p<0.0001, **, p<0.01). **(D) Scd1 localization to the old end is not impaired in *gef1Δ*.** Quantification of Scd1-3xGFP localization to old ends in *gef1+* and *gef1Δ cells*. Reported p values from Student's t-tests. n.s. = not significant. Cell division site, CDS.

Supplemental Figure 3

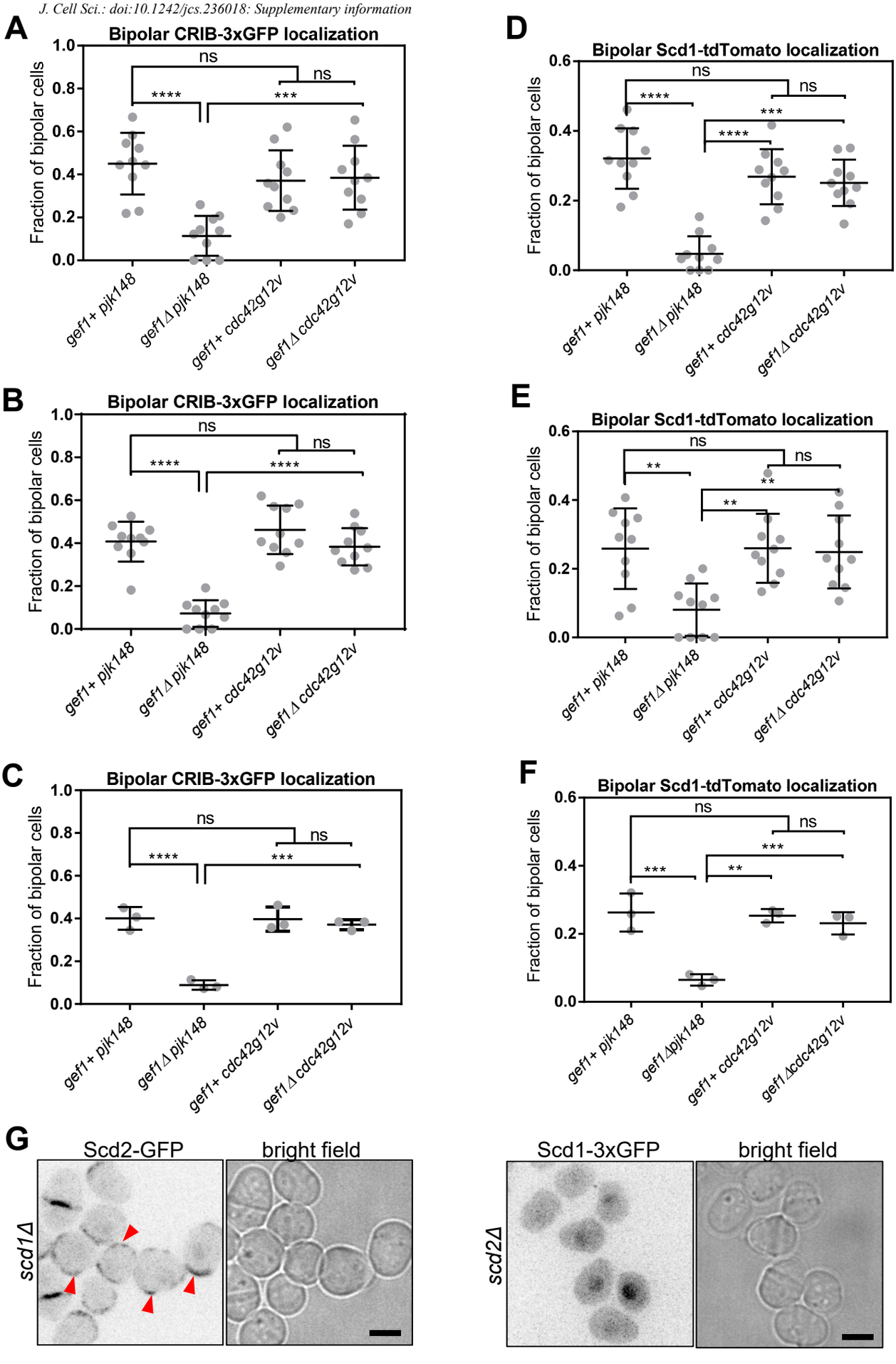

Supplemental Figure 4

Figure S4: (A-F) Gef1-mediated Cdc42 activation promotes bipolar CRIB and Scd1 localization. (A and B) Quantification of 2 additional independent replicates of the experiment depicted in Fig. 5A,B. **(C)** Quantification of the means from all 3 replicate experiments. **(D and E)** Quantification of 2 additional independent replicates of the experiment depicted in Fig. 5A,C. **(F)** Quantification of the means from all 3 replicate experiments. All data points are plotted in each graph, with black bars on top of data points that show the mean and standard deviation for each genotype. Each data point corresponds to the mean of an analyzed field of cells (n>5) from the same experiment. Significance determined by one-way ANOVA with Tukey's multiple comparisons post hoc test (****, p<0.0001, ***, p<0.001, **, p<0.01, ns, not significant). **(G) Scd1 requires *scd2* to localize to the CDS and the cortex, but Scd2 localization is unimpaired in the absence of *scd1*.** Scd2-GFP and Scd1- 3xGFP localization to the cortex in *scd1Δ* and *scd2Δ* cells, respectively. Red arrowheads indicate cells with Scd2-GFP localized tot the cell cortex

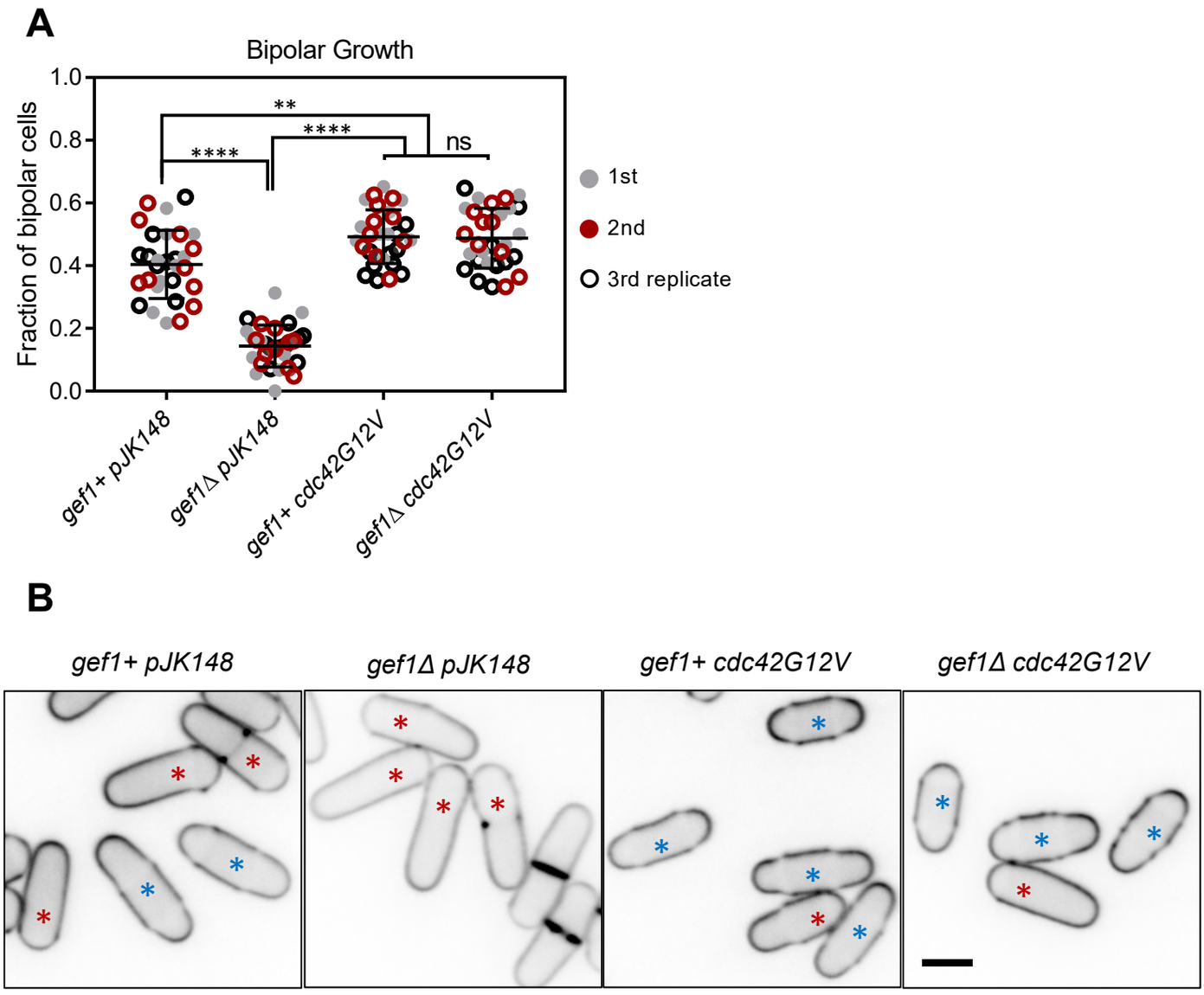

Figure S5: Gef1 promotes the transition to bipolar growth. (A) Quantification of the percentage of cells exhibiting bipolar growth in the indicated genotypes. Red, grey, and black circles identify the replicate to which each data point belongs. **(B)** Representative images of calcofluor stained cells of the indicated genotypes. Red and blue asterisks denote monopolar and bipolar cells, respectively. All data points are plotted in each graph, with black bars on top of data points that show the mean and standard deviation for each genotype. Each data point corresponds to the mean of an analyzed field of cells (n>5) from the same experiment. Significance determined by one-way ANOVA with Tukey's multiple comparisons post hoc test (****, p<0.0001, **, p<0.01, ns, not significant). Scale bar=5μm.

Supplemental Figure 5

A

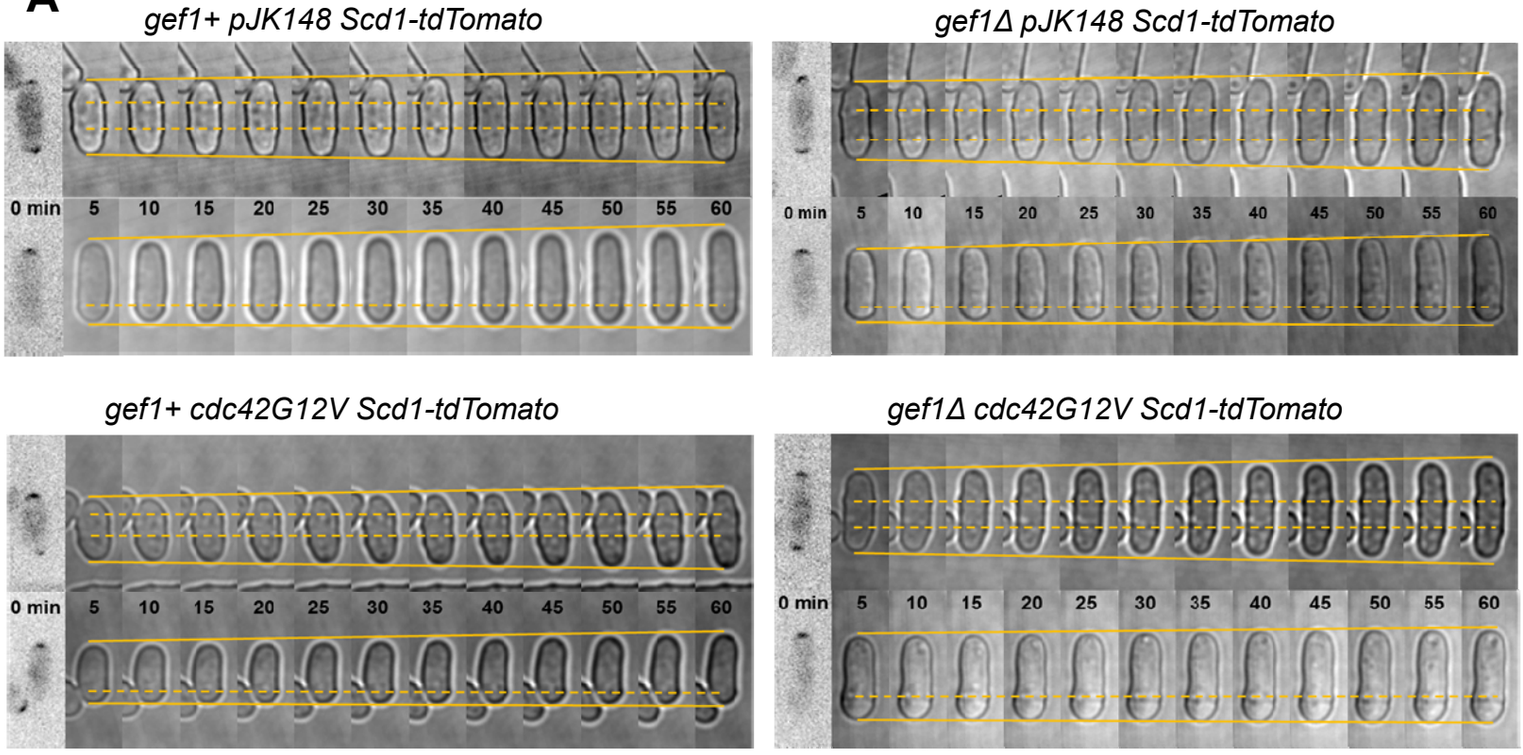

B

	% of cells with bipolar Scd1 that grow from both ends	% of cells with monopolar Scd1 that grow only from that end	% of cells with monopolar Scd1 that grow from both ends
gef1+ pJK148 N=34	100%	79%	21%
gef1Δ pJK148 N=24	100%	91%	9%
gef1+ cdc42G12V N=29	100%	81%	19%
gef1Δ cdc42G12V N=29	100%	80%	20%

Figure S6: Growth pattern of cells corresponding to tip localization of Scd1. (A) Montages monitoring growth over time from cells with monopolar or bipolar Scd1-tdTomato localization at movie time t0 in the indicated genotypes. Dashed lines mark the birth scar(s) used to measure tip growth, shown by sloped solid lines. Non growing ends indicated by solid lines that are parallel to the dashed reference lines. **(B)** Table detailing the growth pattern of cells with respect to initial Scd1 localization. Scale bar=5μm.

Supplemental Figure 6

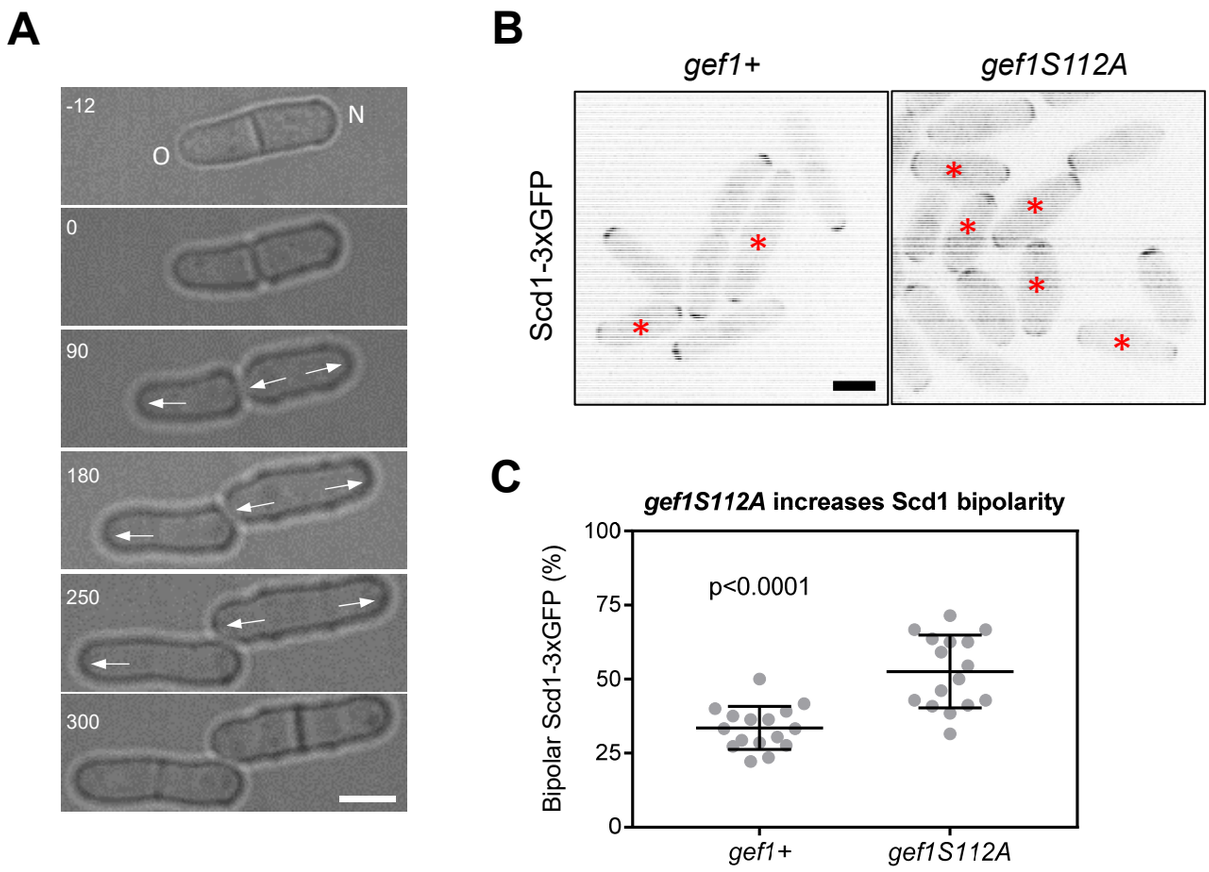

Figure S7: (A) Growth pattern in the progeny of a monopolar *gef1Δ* cell. Image at -12 mins shows a monopolar *gef1Δ* cell that in the previous generation grew only from the old end (O) while the new end (N) did not have any prior history of growth. Time stamps are minutes elapsed since completion of division. Arrows indicate direction of growth at cell ends. **(B and C) Gef1 promotes the transition to bipolar growth. (B)** Localization of Scd1-3xGFP to the cell poles in *gef1+* and *gef1S112A* cells. Asterisks indicate cells with bipolar Scd1-3xGFP localization. **(C)** Quantification of the percent of cells that exhibit bipolar Scd1-3xGFP localization at cell ends in the indicated genotypes. All data points are plotted in each graph, with black bars on top of data points that show the mean and standard deviation for each genotype. Each data point corresponds to the mean of an analyzed field of cells (n>5) from the same experiment. Reported p values from Student's t-tests. Scale bar=5μm.

Supplemental Figure 7

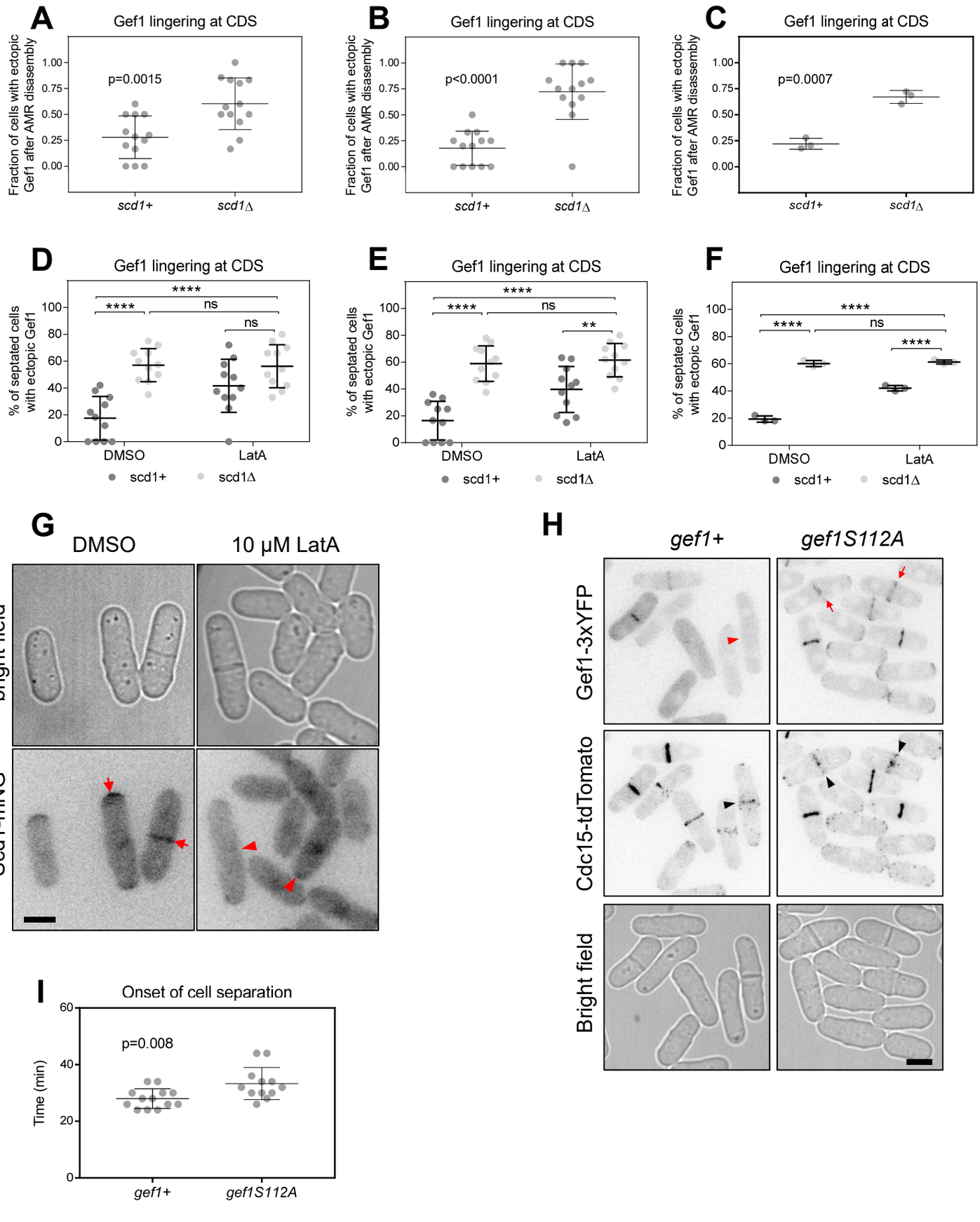

Supplemental Figure 8

Figure S8: (A-F) Scd1 promotes Gef1 removal from the division site. to enable cell separation. (A and B) Quantification of 2 additional independent replicates of the experiment depicted in Fig. 7C,D. **(C)** Quantification of the means from all 3 replicate experiments. **(D and E)** Quantification of 2 additional independent replicates of the experiment depicted in Fig. 7E,F. **(F)** Quantification of the means from all 3 replicate experiments. All data points are plotted in each graph, with black bars on top of data points that show the mean and standard deviation for each genotype. Each data point corresponds to the mean of an analyzed field of cells (n>5) from the same experiment. Significance determined by one-way ANOVA with Tukey's multiple comparisons post hoc test (****, p<0.0001, ***, p<0.001, **, p<0.01, ns, not significant). **(G) Scd1 requires actin for its localization to the CDS and the cortex.** Scd1-mNG localization to the division site and cell tips in cells treated with 10 µM LatA or DMSO. Red arrows indicate cells with Scd1-mNG localized to the CDS or cell tip. Red arrowheads indicate cells where Scd1-mNG fails to localize to the division site or to the cell tips. All images are inverted max projections with the exception of bright field. Scale bars = 5µm. Cell Division Site, CDS. **(H-I) Gef1 removal from the division site promotes cell separation. (H)** Gef1-3YFP and Gef1S112A-3YFP localization in cells expressing the ring marker Cdc15-tdTomato. Red arrow head indicates the absence of Gef1 from the division site after ring constriction. Red arrows indicate the presence of Gef1 at the division site after ring constriction. Black arrow heads mark the division site of cells that have completed ring constriction. **(I)** Quantification of onset of cell separation after completion of ring constriction in *gef1+* and *gef1S112A* cells. Reported p values from Student's t-tests. Scale bar=5µm.

Table S1. Strains list.		
Strain	Genotype	Source
PN567	h+ ade6-704 leu1-32 ura4-d18	Paul Nurse
PN1191	cdc10-129 ade6-704 leu1-32	Paul Nurse
JX125	h90 Δscd1::ura4+ ade6 leu1-32 ura4-d18 h210	(Hirota et al., 2003)
FV1218	Gef1-3xYFP:kanMX ade6-704 leu1-32 ura4-d18	(Das et al., 2009)
YSM947	Scd1-3xGFP:kanMX ade6-m216 leu1-32 ura4-d18	(Bendezu and Martin, 2013)
MBY3451	P3 nmt1:3HA-Shk1:KANr leu1-32 ura4-d18	(Loo and Balasubramanian, 2008)
YMD1172	Scd1-tdTomato:KANr ade6-704 leu1-32 ura4-d18	This study
YMD1256	Δgef1::ura4+ pjk148-nmt41x:cdc42G12V-leu1+ CRIB-3xGFP:ura4+ Scd1-tdTomato:KanMX ade6 leu1-32 ura4-d18	This study
YMD1271	pjk148-nmt41x-leu1+ CRIB-3xGFP:ura4+ Scd1-tdTomato:KanMX ade6 leu1-32 ura4-d18	This study
YMD1273	Δgef1::ura4+ pjk148-nmt41x-leu1+ CRIB-3xGFP:ura4+ Scd1-tdTomato:KanMX ade6 leu1-32 ura4-d18	This study
YMD1232	pjk148-nmt41x:cdc42G12V-leu1+ CRIB-3xGFP:ura4+ Scd1-tdTomato:KanMX ade6 leu1-32 ura4-d18	This study
YMD317	CRIB-3xGFP:ura4+ Rlc1-tdTomato:NATr Sad1-mCherry:kanMX ade6-M21X leu1-32 ura4-D18	(Wei et al., 2016)
YMD432	Δgef1::ura4+ pjk148-nmt41x:cdc42G12V-leu1+ CRIB-3xGFP:ura4+ ade6 leu1-32 ura4-d18	This study
YMD488	Δgef1::ura4+ CRIB-3xGFP:ura4+ Rlc1-tdTomato:NATr Sad1-mCherry:kanMX ade6 leu1-32 ura4-d18	(Wei et al., 2016)
YMD530	h90 Δscd1::ura4+ CRIB-3xGFP:ura4+ Rlc1-tdTomato:NATr Sad1-mCherry:kanMX ade6-M21X leu1-32 ura4-d18	(Wei et al., 2016)
YMD602	pjk148-nmt41x:cdc42G12V-leu1+ CRIB-3xGFP:ura4+ ade6 leu1-32 ura4-d18	This study
YMD1043	Gef1-tdTomato:KANr Scd2-GFP:KANr ade6 leu1-32 ura4-d18	This study
YMD1204	Scd1-tdTomato:KANr Scd2-GFP:KANr ade6 leu1-32 ura4-d18	This study

YMD1049	Scd1-3xGFP:KANr Gef1-tdTomato:KANr ade6 leu1-32 ura4-d18	This study
YMD761	Δgef1::ura4+ Scd1-3xGFP:kanMX Rlc1-tdTomato:NATr Sad1-mCherry:kanMX ade6-m216 leu1-32 ura4-d18	This study
YMD773	Scd1-3xGFP:kanMX Rlc1-tdTomato:NATr Sad1-mCherry:kanMX ade6-m216 leu1-32 ura4-d18	This study
YMD795	nmt1:3HA-Shk1 scd2-GFP:kanMX	This study
YMD840	Δgef1::ura4+ Scd2-GFP:kanMX Rlc1-tdTomato:NATr Sad1-mCherry:kanMX ade6 leu1-32 ura4-d18	This study
YMD842	Scd2-GFP:kanMX Rlc1-tdTomato:NATr Sad1-mCherry:kanMX kanMX ade6 leu1-32 ura4-d18	This study
YMD910	Gef1-NeonGreen:kanMX leu1-32 ura4-d18	This study
YMD926	Gef1-NeonGreen:kanMX Rlc1-tdTomato:NATr Sad1-mCherry:kanMX ade6 leu1-32 ura4-d18	This study
YMD936	Δgef1::ura4+ pjk148-nmt41x:cdc42G12V-leu1+ Scd1-3xGFP:kanMX ade6-m216 leu1-32 ura4-d18	This study
YMD994	pjk148-nmt41x:cdc42G12V-leu1+ Scd1-3xGFP:kanMX ade6-m216 leu1-32 ura4-d18	This study
YMD996	h90 Δscd1::ura4+ Scd2-GFP:kanMX Rlc1-tdTomato:NATr ade6 leu1-32 ura4-d18	This study
YMD998	pjk148-nmt41x-leu1+ CRIB-3xGFP:ura4+ ade6 leu1-32 ura4-d18	This study
YMD1000	Δgef1::ura4+ pjk148-nmt41x-leu1+ CRIB-3xGFP:ura4+ ade6 leu1-32 ura4-d18	This study
YMD1002	Δgef1::ura4+ pjk148-nmt41x-leu1+ Scd1-3xGFP:kanMX ade6-m216 leu1-32 ura4-d18	This study
YMD1004	pjk148-nmt41x-leu1+ Scd1-3xGFP:kanMX ade6-m216 leu1-32 ura4-d18	This study
YMD1030	h90 Δscd1::ura4+ Gef1-NeonGreen:kanMX Rlc1-tdTomato:NATr Sad1-mCherry:kanMX ade6 leu1-32 ura4-d18	This study
YMD1067	h90 Δscd2::ura4+ Gef1-NeonGreen:kanMX Sad1-mCherry:kanMX ade6 leu1-32 ura4-d18 h210	This study
YMD1069	h90 Δscd2::ura4+ Scd1-3xGFP:kanMX Rlc1-tdTomato:NATr ade6-m216 leu1-32 ura4-d18	This study
YMD1088	gef1s112a:kanMX Scd1-3xGFP:kanMX ade6-m216 leu1-32 ura4-d18	This study
YMD965	Δgef1::ura4+ gef1S112A-3xYFP:kanMX Cdc15-tdTomato:Nat^r ade6 leu1-32 ura4-d18	This study
YMD208	Cdc15-tdTomato:NAT^r Gef1-3xYFP:kanMX ade6	(Wei et al., 2016)

REFERENCES:

Bendezu, F.O., and S.G. Martin. 2013. Cdc42 explores the cell periphery for mate selection in fission yeast. *Curr Biol*. 23:42-47.

Das, M., D.J. Wiley, X. Chen, K. Shah, and F. Verde. 2009. The conserved NDR kinase Orb6 controls polarized cell growth by spatial regulation of the small GTPase Cdc42. *Curr Biol*. 19:1314-1319.

Hirota, K., K. Tanaka, K. Ohta, and M. Yamamoto. 2003. Gef1p and Scd1p, the Two GDP-GTP exchange factors for Cdc42p, form a ring structure that shrinks during cytokinesis in Schizosaccharomyces pombe. *Mol Biol Cell*. 14:3617-3627.

Loo, T.H., and M. Balasubramanian. 2008. Schizosaccharomyces pombe Pak-related protein, Pak1p/Orb2p, phosphorylates myosin regulatory light chain to inhibit cytokinesis. *J Cell Biol*. 183:785-793.

Wei, B., B.S. Hercyk, N. Mattson, A. Mohammadi, J. Rich, E. DeBruyne, M.M. Clark, and M. Das. 2016. Unique spatiotemporal activation pattern of Cdc42 by Gef1 and Scd1 promotes different events during cytokinesis. *Mol Biol Cell*. 27:1235-1245.